J. Fluid Mech. (2002), *vol.* 456, *pp.* 377–409.
DOI: 10.1017/S0022112002007759 Printed in the United Kingdom

Amplification of energy flux of nonlinear acoustic waves in a gas-filled tube under an axial temperature gradient

By N. SUGIMOTO AND K. TSUJIMOTO

Department of Mechanical Science, Graduate School of Engineering Science, University of Osaka, Toyonaka, Osaka 560-8531, Japan

(Received 24 May 2001 and in revised form 30 October 2001)

This paper considers nonlinear acoustic waves propagating unidirectionally in a gas-filled tube under an axial temperature gradient, and examines whether the energy flux of the waves can be amplified by thermoacoustic effects. An array of Helmholtz resonators is connected to the tube axially to avoid shock formation which would otherwise give rise to nonlinear damping of the energy flux. The amplification is expected to be caused by action of the boundary layer doing reverse work, in the presence of the temperature gradient, on the acoustic main flow outside the boundary layer. By the linear theory, the velocity at the edge of the boundary layer is given in terms of the fractional derivatives of the axial velocity of the gas in the acoustic main flow. It is clearly seen how the temperature gradient controls the velocity at the edge. The velocity is almost in phase with the heat flux into the boundary layer from the wall. With effects of both the boundary layer and the array of resonators taken into account, nonlinear wave equations for unidirectional propagation in the tube are derived. Assuming a constant temperature gradient along the tube, the evolution of compression pulses is solved numerically by imposing the initial profiles of both an acoustic solitary wave and of a square pulse. It is revealed that when a positive gradient is imposed, the excess pressure decreases while the particle velocity increases and that the total energy flux can indeed be amplified if the gradient is suitable.

1. Introduction

Nonlinear acoustic waves propagating in a gas-filled tube generally tend to evolve into a shock as the magnitude of pressure disturbances becomes large. When the shock emerges, it gives rise to nonlinear damping in addition to linear damping, due mainly to wall friction through a boundary layer. Then the energy flux carried by the waves decays significantly. In this sense, intense compression pulses are commonly incapable of transferring energy over a long distance.

It has recently been revealed, however, that shock-free propagation can be achieved by connecting a suitable array of Helmholtz resonators to the tube axially (Sugimoto 1992). Particularly in the lossless limit, an acoustic solitary wave without a shock can propagate without any change of form at a constant subsonic speed (Sugimoto 1996; Sugimoto *et al.* 1999). The solitary wave is the compression pulse and it can convey energy steadily, as well as mass and momentum (Sugimoto 2000). In reality, however, the solitary wave is subjected to linear damping due to wall friction and also diffusivity of sound. But it would be interesting to know if the total energy can be maintained against the loss effects or can even be amplified, which would find many

applications. To achieve this, we consider exploitation of thermoacousitc effects by imposing a temperature gradient along the tube.

When a temperature gradient is present, there are two effects involved in propagation: one is a lossless effect due to non-uniformity in the equilibrium state and the other is a loss effect due to the boundary layer. For the former, it has already been shown that the excess pressure and the particle velocity behave oppositely, as $-1/4$ and $+1/4$ powers of the local equilibrium temperature, respectively, so that the energy flux is kept constant (Sugimoto & Tsujimoto 2001). This power law is a consequence of the geometrical acoustics, i.e. the conservation of energy flux over a ray tube (Pierce 1991). The ray tube in the present case is the tube itself so that the cross-sectional area is constant, and the acoustic impedance decreases in proportion to the inverse of the square root of the local equilibrium temperature. While such a law is valid in the short-term, the solitary wave gives rise to fission or oscillatory tails in the long-term. Taking full account of both the lossless and loss effects, this paper examines propagation of not only the solitary wave but also a smoothed square pulse to examine the feasibility of amplification of the energy flux.

Acoustic waves interacting with a solid boundary in a temperature gradient have provided many interesting thermoacoustic phenomena. They have recently attracted much attention from the viewpoint of realizing thermoacoustic heat engines (Wheatley 1986; Swift 1988, 1995; Yazaki *et al.* 1998; Backhaus & Swift 1999). In general, however, thermoacousitc phenomena do not seem to be understood clearly even from the standpoint of the linear theory of fluid dynamics. This is because the boundary layer exhibits a hereditary (or memory) effect even in a Newtonian fluid, which gives rise to a phase lag of multiples of $\pm\pi/4$ for a harmonic wave. This intermediate phase lag has obscured intuitive understanding of the phenomena. But use of fractional calculus will resolve this problem to some extent.

The boundary layer including the heat conduction was treated first by Kirchhoff (1868) for a time-harmonic disturbance and later extended by Chester (1964) to a general disturbance. In the context of the thermoacoustics where a temperature gradient is present on the wall, Rott (1969, 1973) has developed a theory to examine the conditions of the onset of self-excited oscillations. In the spirit of Kirchhoff, Chester and Rott and assuming a general disturbance, the linear theory of the boundary layer is developed here by using fractional calculus. It is shown that the velocity v_b at the edge of the boundary layer directed away from the wall (see figure 1) is given by

$$v_b = -\left(1+\frac{\gamma-1}{\sqrt{Pr}}\right)\frac{\sqrt{\nu_e}}{\rho_e a_e^2}\frac{\partial^{1/2}p'}{\partial t^{1/2}} + \left(\frac{1}{2}+\frac{1}{\sqrt{Pr}+Pr}\right)\frac{\sqrt{\nu_e}}{T_e}\frac{\mathrm{d}T_e}{\mathrm{d}x}\frac{\partial^{-1/2}u}{\partial t^{-1/2}}, \tag{1.1}$$

where $p'(x,t)$ and $u(x,t)$ denote, respectively, the excess pressure and the particle velocity parallel to the wall outside the boundary layer, called the acoustic main flow, x and t being the axial coordinate and the time, respectively; $\rho_e(x)$, $T_e(x)$, $\nu_e(x)$ and $a_e(x)$ denote, respectively, the density of the gas in the local equilibrium state, the wall temperature, the kinematic viscosity and the linear sound speed, γ and Pr being the ratio of the specific heats and the Prandtl number. Here the fractional derivatives of order α ($\alpha=-1/2$ or $1/2$) of a function $f(x,t)$ are defined as (see e.g. Sugimoto 1989)

$$\frac{\partial^\alpha f}{\partial t^\alpha} = \frac{1}{\sqrt{\pi}}\int_{-\infty}^{t}\frac{1}{\sqrt{t-\tau}}\frac{\partial^{\alpha+1/2}}{\partial\tau^{\alpha+1/2}}f(x,\tau)\mathrm{d}\tau. \tag{1.2}$$

The relation (1.1) generalizes Rott's result (Rott 1980, equation (2.20) with $n=1$ and

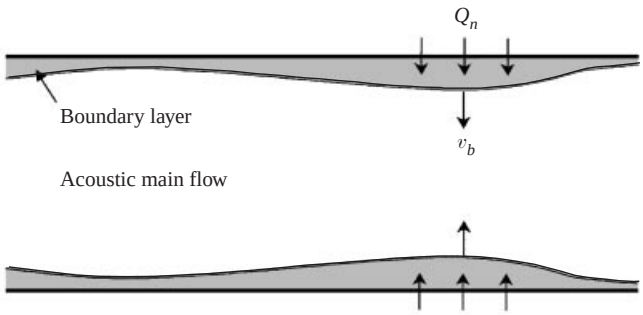

FIGURE 1. Illustration of the region of the acoustic main flow and the boundary layer (exaggerated in scale) in the tube where v_b and Q_n represent, respectively, the velocity at the edge of the boundary layer directed into the main-flow region and the heat flux into the boundary layer through the wall.

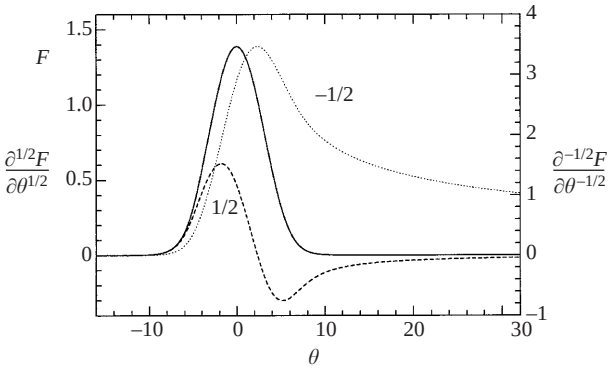

FIGURE 2. Profiles of the compression pulse F and of its fractional derivatives where the solid line represents $F(\theta)$, which is the profile of the acoustic solitary wave given by (6.15) with $s = 0.5$, while the broken and dotted lines represent profiles of its fractional derivatives of order $1/2$ and $-1/2$, respectively.

$\beta = 0$) derived in the case of a harmonic oscillation to include a general type of disturbance.

By using this, we first consider how the energy of acoustic waves is lost in propagation. In the absence of the temperature gradient, the second term in v_b drops out. Imagine the propagation of the compression pulse drawn as the solid line in figure 2, where F and θ denote p' and t, respectively and F is an even function. As shown in the detailed explanation given in § 6.1, F is the pressure profile of the acoustic solitary wave. The $1/2$-order derivative of F is depicted as the broken line. It is characteristic that the derivative is no longer even or odd but asymmetric with respect to $\theta = 0$ and that a slowly decreasing tail appears. Looking at a fixed point in a boundary layer when the pulse passes by, it is seen that v_b is first negative so that the region of the acoustic main flow, i.e. the pulse, pushes the boundary layer toward the wall. In other words, the pulse does work $-p'v_b$ on the boundary layer per unit time. But because v_b changes sign as t increases, the boundary layer recoils to push back the pulse. The recoil is the hereditary effect of the boundary layer. In this case, the boundary layer does work on the pulse. From the graphs of figure 2, however, the integration of $-p'v_b$ over the time, i.e. of $F\partial^{1/2}F/\partial\theta^{1/2}$ over θ, is seen to be positive. Therefore it follows that the pulse has done net work outward. If v_b were given by

the first-order derivative of p', the integral would vanish and no net work would be done. This difference is the essence of the action of the boundary layer. When the pulse continues to do work outward, as is physically the case, its energy is lost so that the pulse eventually decays.

If a temperature gradient is present, the second term in v_b comes into play. Since u is proportional to p' for a wave travelling unidirectionally and the ratio p'/u is the acoustic impedance $\rho_e a_e$, the second term is given by the derivative of p' of $-1/2$-order. The explicit form of the derivative of $-1/2$-order is depicted in figure 2 in the dotted line where the algebraically decaying long tail is typical. From the definition, the derivative always takes a positive value as long as p' is positive. Therefore if the temperature gradient $\mathrm{d}T_e/\mathrm{d}x$ is positive and steep enough, v_b will become positive when the excess pressure in the main flow is positive. This means that the boundary layer does work on the main flow. If this condition continues to be met afterwards, then the energy flux of the main flow tends to be increased. This is the mechanism of amplification. It is also shown that v_b is almost in phase with the heat flux from the wall into the boundary layer. Therefore amplification occurs if the heat flux is into (or out of) the boundary layer when p' is positive (or negative). This is a restatement of Rayleigh's (necessary) criterion of the onset of instability: at the phase of greatest condensation, heat is received by the air and at the phase of great rarefaction heat is given up from it, and thus there is a tendency to maintain the vibrations (Rayleigh 1945).

Incidentally, in the case of a time-harmonic disturbance p' in the form of $\exp(\mathrm{i}\omega t)$, the derivative of $-1/2$-order is reduced to the Fresnel integrals (see e.g. Abramowitz & Stegun 1972) and is evaluated as $2^{-1/2}(1-\mathrm{i})\exp(\mathrm{i}\omega t) = (\mathrm{i}\omega)^{-1/2}\exp(\mathrm{i}\omega t)$. Thus the derivative of $-1/2$-order lags in phase by $\pi/4$. The derivative of $1/2$-order is defined by differentiating it with respect to t once and therefore is given by $(\mathrm{i}\omega)^{1/2}\exp(\mathrm{i}\omega t)$ so that it is greater by $\pi/4$. For a harmonic travelling wave in the positive direction of x, u in (1.1) may be replaced by $p'/\rho_e a_e$ and the condition for local amplification that the integral of $p'v_b$ over one period should be positive is imposed on the temperature gradient. It is easily shown that the gradient is required to be positive and to satisfy the inequality $T_e^{-1}\mathrm{d}T_e/\mathrm{d}x > \Gamma\omega/a_e$ to overcome the wall friction, where $\Gamma = 2(\gamma - 1 + \sqrt{Pr})(1 + \sqrt{Pr})/(2 + \sqrt{Pr} + Pr)$. The condition of a positive gradient agrees quantitatively with the experimental result by Yazaki *et al.* (1998). For a standing wave, u in (1.1) is related to a spatial gradient of p' and the condition for local amplification depends on the location x. In fact, the condition is given by $(T_e^{-1}\mathrm{d}T_e/\mathrm{d}x)(|P|^{-1}\mathrm{d}|P|/\mathrm{d}x) > \Gamma\omega^2/a_e^2$, $P(x)$ being a complex amplitude of the excess pressure (see also Howe 1998†).

In what follows, we start by presenting the basic equations and considering the equilibrium state for the temperature gradient on the tube wall in § 2. The acoustic main flow outside the boundary layer is formulated in § 3 where the wave equations describing the bidirectional propagation are derived by taking account of the nonlinearity, the boundary layer and the weak diffusivity of sound. The effect of the boundary layer appears through v_b only. To relate v_b with the quantities in the acoustic main flow, the linear theory of the boundary layer is developed in § 4 and v_b is given by (1.1). The equation for the array of resonators couples with the equations for the main flow in just the same way as v_b. Focusing on unidirectional propagation, § 5 is devoted to derivation of the simplified nonlinear wave equations and to consideration

† This condition reduces to Howe's result (6.5.5) if the dependence of v_e on x is ignored, i.e. the factor $1/2$ in the second term of (1.1) (which results from $\partial\hat{u}/\partial x$ in (A 5) of Appendix A) is omitted.

of the properties of the equations. In § 6, amplification of the energy flux is examined by solving the evolution of an acoustic solitary wave and of a square pulse in the case of a positive, constant temperature gradient. Some discussion is given on the results. Finally, in Appendix B an example of initial-value problems in the linear case is solved to provide a qualitative understanding of effects due to the wall friction and the temperature gradient on wave propagation.

2. Basic equations and equilibrium state

This section presents the basic equations to be used for the analysis in the following sections and considers the equilibrium state in the case of no gravity. The basic equations consist of the equations of continuity, momentum and energy as follows:

$$\frac{\partial \rho}{\partial t} + \nabla \cdot (\rho \boldsymbol{v}) = 0, \tag{2.1}$$

$$\rho \frac{\mathrm{D}\boldsymbol{v}}{\mathrm{D}t} = -\nabla p + \mu \Delta \boldsymbol{v} + (\mu_v + \tfrac{1}{3}\mu)\nabla \nabla \cdot \boldsymbol{v}, \tag{2.2}$$

$$\rho T \frac{\mathrm{D}S}{\mathrm{D}t} = k \Delta T + \Phi, \tag{2.3}$$

with $\mathrm{D}/\mathrm{D}t = \partial/\partial t + \boldsymbol{v} \cdot \nabla$ where ρ, $\boldsymbol{v}$, p, T and S denote, respectively, density, velocity vector, pressure, temperature and entropy, and Φ denotes the viscous dissipation function quadratic in the rate of strain; μ, μ_v and k denote, respectively, the coefficients of the shear and bulk viscosities and the thermal conductivity. The dependence of these material constants on temperature is ignored for simplicity and they are taken to be constants. Equations (2.1) to (2.3) are supplemented by the two equations of state which account for the thermodynamic quantities by two independent variables. Assuming an ideal gas, the pressure is expressed in terms of the density and the temperature as

$$\frac{p}{p_0} = \frac{\rho T}{\rho_0 T_0}, \tag{2.4}$$

with $p_0 = \mathscr{R}\rho_0 T_0$, $\mathscr{R}$ being the gas constant, where the subscript 0 for ρ, p, T (and S below) denotes the respective constant values in the reference equilibrium state. The pressure can alternatively be expressed in terms of ρ and S as

$$\frac{p}{p_0} = \left(\frac{\rho}{\rho_0}\right)^{\gamma} \exp\left(\frac{S - S_0}{c_v}\right), \tag{2.5}$$

with $\gamma = c_p/c_v$ where c_p and c_v are specific heats at constant pressure and volume, respectively.

We next consider the equilibrium state of the gas in the tube when the wall temperature is kept constant temporally but varied in the axial direction. In the quiescent state $\boldsymbol{v} = 0$, p must be uniform throughout the tube, i.e. $p = p_0$. The steady field of the temperature must satisfy the Laplace equation from (2.3):

$$\Delta T = 0. \tag{2.6}$$

Taking the x-axis in the axial direction of the tube, and the y- and z-axes in the plane normal to the x-axis, and denoting the wall temperature by $T_w(x)$, we seek the equilibrium temperature of the gas, denoted by T_e, in the form of the sum

$T_e = T_w(x) + \Theta(x, y, z)$. It then follows from (2.6) that

$$\frac{\partial^2 \Theta}{\partial x^2} + \frac{\partial^2 \Theta}{\partial y^2} + \frac{\partial^2 \Theta}{\partial z^2} = -\frac{\mathrm{d}^2 T_w}{\mathrm{d}x^2}. \tag{2.7}$$

We assume that a typical axial length l in the variation of the wall temperature is much longer than a typical diameter of the tube such that

$$\left|\frac{\partial^2 \Theta}{\partial x^2}\right| \ll \left|\frac{\partial^2 \Theta}{\partial y^2}\right|, \ \left|\frac{\partial^2 \Theta}{\partial z^2}\right|. \tag{2.8}$$

By this assumption, the first term on the left-hand side of (2.7) is ignored. For a circular tube of radius R, the axisymmetric temperature field is then

$$\Theta(r, x) = \frac{1}{4}\frac{\mathrm{d}^2 T_w}{\mathrm{d}x^2}(R^2 - r^2), \tag{2.9}$$

where r is the radial coordinate from the centre axis. The mean temperature $\bar{T}_e$ over the cross-section of the tube is given by

$$\bar{T}_e = \frac{1}{\pi R^2}\int_0^R 2\pi r T_e \mathrm{d}r = T_w + \frac{R^2}{8}\frac{\mathrm{d}^2 T_w}{\mathrm{d}x^2}. \tag{2.10}$$

It is found from this that $\bar{T}_e$ differs from T_w by the second term on the right-hand side.

Since $R \ll l$, the magnitudes of the derivatives of T_w are ordered as

$$R^2\left|\frac{\mathrm{d}^2 T_w}{\mathrm{d}x^2}\right| \ll R\left|\frac{\mathrm{d}T_w}{\mathrm{d}x}\right| \ll |T_w|. \tag{2.11}$$

In the following sections, variations of T_w are taken into account up to the first-order derivative and the second-order one is neglected. Then T_e is substantially equal to T_w, which is regarded as being linear with respect to x. Also the steady heat flux through the wall $-k\partial T_e/\partial r$ is neglected and the heat flux exists only axially in the tube, i.e. $-k\partial T_e/\partial x$. We note that if T_w is strictly linear, its second-order derivative vanishes automatically so that no approximations are involved.

The above approximation stipulates that the temperature of the gas in equilibrium is equal to that of the wall and uniform over the cross-section of the tube. So the overbar on T_e is removed hereafter. Correspondingly the density, temperature and entropy in the equilibrium state vary in the axial direction only. This dependence is indicated by the subscript e. From (2.4) and (2.5), $\rho_e(x)$, $T_e(x)$ and $S_e(x)$ must satisfy

$$\frac{\rho_e T_e}{\rho_0 T_0} = 1, \tag{2.12}$$

and

$$\left(\frac{\rho_e}{\rho_0}\right)^{\gamma} \exp\left(\frac{S_e - S_0}{c_v}\right) = 1. \tag{2.13}$$

3. Formulation of the acoustic main flow

Propagation of nonlinear acoustic waves is characterized by the acoustic Mach number ε and the acoustic Reynolds number Re defined, respectively, as

$$\varepsilon = \frac{u_0}{a_0} \ll 1, \quad \frac{1}{Re} = \frac{\nu\omega}{a_0^2} \ll 1, \tag{3.1}$$

where u_0 and a_0 denote, respectively, a typical speed of gas and a typical sound speed, while ν $(= \mu/\rho)$ denotes the kinematic viscosity of the gas, ω being a typical angular frequency. While Re is defined in reference to the sound speed and a typical wavelength a_0/ω, the Reynolds number referred to the flow induced, Re_f, may be defined as $a_0 u_0/\nu\omega$, which is equal to εRe and so smaller by ε. We assume that the acoustic Mach number is small but finite for quadratically nonlinear theory to be required but the Reynolds number Re_f is still large enough for dissipative effects to be secondary except in a boundary layer, and a shock layer if any.

A typical thickness of the boundary layer is estimated to be $(\nu/\omega)^{1/2}$. This is assumed to be much smaller than the radius of the tube:

$$\frac{(\nu/\omega)^{1/2}}{R} = \frac{1}{Re^{1/2}} \frac{a_0/\omega}{R} \ll 1. \tag{3.2}$$

By this, the smallness of $1/Re$ may be limited in relation to the ratio of the wavelength a_0/ω to the radius R, where the former is assumed, of course, to be much longer than the latter. In addition, a typical axial length l of the temperature variations is assumed to be much longer than the typical wavelength ($R \ll a_0/\omega \ll l$). This is designated by a small parameter χ:

$$\chi = \frac{a_0/\omega}{l} \ll 1. \tag{3.3}$$

Under these assumptions, we define the region of acoustic main flow in the tube as that excluding the thin boundary layer on the wall and the vicinity of the orifices from the resonators. In this region, quasi-one-dimensional propagation can be assumed. The acoustic main flow is formulated in the same manner as previously (Sugimoto 1992) except for treatment of the temperature variations in the equilibrium state. Therefore the description here is kept to a minimum and readers are referred to that paper for details.

Because of the presence of the boundary layer and the resonators, the acoustic main flow deviates slightly from being rigorously one-dimensional. Let a physical quantity in the region be given by the sum of a mean value over the cross-section of the region and a small deviation from it, and let the basic equations presented in the preceding section be averaged over the cross-section. We take into account all terms up to the first order of the deviation. But we ignore the first-order deviation when multiplied by the viscosity or the thermal conductivity, since the dissipative effects are small. The deviation taken into account in the following is due solely to v_n, which is the velocity v_b at the edge of the boundary layer where the tube wall exists or the velocity $-w$ of the flow into the tube from the resonator where there are orifices in the wall. Hereafter the quantities ρ, u, p, T and S should be understood as the mean values after being averaged, so they are regarded as functions of x and t only.

The equation of continuity is given by

$$\frac{\partial \rho}{\partial t} + \frac{\partial}{\partial x}(\rho u) = \frac{1}{A} \oint \rho v_n \mathrm{d}s, \tag{3.4}$$

where $A(x, t)$ is the cross-sectional area of the main-flow region and is dependent on x and t, but no distinction from the constant cross-sectional area of the tube itself will be made because the difference is small and higher order. The integral is taken along the boundary of the main-flow region, ds being a line element along it. The equation of momentum in the axial direction and the equation of energy take, respectively, the

same form as those in the one-dimensional case:

$$\frac{\partial u}{\partial t}+u\frac{\partial u}{\partial x}=-\frac{1}{\rho}\frac{\partial p}{\partial x}+\frac{1}{\rho}(\tfrac{4}{3}\mu+\mu_v)\frac{\partial^2 u}{\partial x^2}, \tag{3.5}$$

and

$$\rho T\left(\frac{\partial S}{\partial t}+u\frac{\partial S}{\partial x}\right)=k\frac{\partial^2 T}{\partial x^2}+(\tfrac{4}{3}\mu+\mu_v)\left(\frac{\partial u}{\partial x}\right)^2. \tag{3.6}$$

In view of (2.12) and (2.13), the equations of state (2.4) and (2.5) are expressed with reference to the local equilibrium values dependent of x as

$$\frac{p}{p_0}=\frac{\rho}{\rho_e}\frac{T}{T_e}, \tag{3.7}$$

and

$$\frac{p}{p_0}=\left(\frac{\rho}{\rho_e}\right)^{\gamma}\exp\left(\frac{S-S_e}{c_v}\right). \tag{3.8}$$

In the following, (3.7) and (3.8) are employed as the equations of state.

The conditions (3.1) assume that effects of nonlinearity and dissipation due to viscosity and heat conduction (if Pr $(=\mu c_p/k)$ is of order unity) are small in the acoustic main flow. Then it is governed, to the lowest approximation, by the linearized and lossless versions of (3.4) and (3.5). But because those small effects will be accumulated during propagation, they tend to become significant over long time and space scales. We now estimate the dissipative effects. The viscous term is apparently present in (3.5) while the effect of heat conduction gives rise to entropy change in (3.6), which appears through the pressure gradient in (3.5). The small entropy change is governed by the energy equation (3.6), which may be linearized about the local equilibrium values by setting $\rho=\rho_e+\rho'$, $T=T_e+T'$ and $S=S_e+S'$ as

$$\frac{\partial S'}{\partial t}+u\frac{\mathrm{d}S_e}{\mathrm{d}x}=\frac{k}{\rho_e T_e}\frac{\partial^2 T'}{\partial x^2}, \tag{3.9}$$

where the quantities with a prime are so small compared with the respective leading terms that their quadratic terms may be neglected, u being designated without prime, and $\mathrm{d}^2T_e/\mathrm{d}x^2$ is neglected by assumption. It is noted that the entropy changes not only through the thermal diffusion on the right-hand side of (3.9) but also by the convection of the second term on the left-hand side. Splitting S' into the convective part S'_c and the diffusive part S'_d, i.e. $S'=S'_c+S'_d$, the respective temporal variations are governed by

$$\frac{\partial S'_c}{\partial t}=-u\frac{\mathrm{d}S_e}{\mathrm{d}x}, \tag{3.10}$$

and

$$\frac{\partial S'_d}{\partial t}=\frac{k}{\rho_e T_e}\frac{\partial^2 T'}{\partial x^2}, \tag{3.11}$$

where $\mathrm{d}S_e/\mathrm{d}x$ is related to the temperature gradient by using (2.12) and (2.13) as

$$\frac{\mathrm{d}S_e}{\mathrm{d}x}=-\frac{c_p}{\rho_e}\frac{\mathrm{d}\rho_e}{\mathrm{d}x}=\frac{c_p}{T_e}\frac{\mathrm{d}T_e}{\mathrm{d}x}. \tag{3.12}$$

We now relate S'_d to u. Equations (3.7) and (3.8) are linearized to yield

$$\frac{p'}{p_0}=\frac{\gamma\rho'}{\rho_e}+\frac{S'}{c_v},\quad \frac{T'}{T_e}=(\gamma-1)\frac{\rho'}{\rho_e}+\frac{S'}{c_v}, \tag{3.13}$$

with $p' = p - p_0$. Here note that the entropy change S'/c_v is much smaller than ρ'/ρ_e and T'/T_e, which are of order ε, because (3.10) and (3.11) indicate that S_c' and S_d' are proportional to the temperature gradient (see (3.12)) and the thermal conductivity, respectively. By using (3.12), S_c'/c_v is estimated to be of order $\chi\varepsilon$ while S_d'/c_v will be estimated by (3.18) to be of order $\varepsilon/PrRe$. Because $1/Re$ is much smaller than χ, S' is mainly due to S_c'.

Linearization of (3.5) with neglect of the viscous term leads to

$$\frac{\partial u}{\partial t} = -\frac{1}{\rho_e}\frac{\partial p'}{\partial x} = -a_e^2\frac{\partial}{\partial x}\left(\frac{\rho'}{\rho_e}\right) - \frac{p_0}{\rho_e}\frac{\partial}{\partial x}\left(\frac{S'}{c_v}\right), \tag{3.14}$$

where a_e is the linear adiabatic sound speed defined by

$$a_e = \left(\frac{\gamma p_0}{\rho_e}\right)^{1/2} = (\gamma \mathscr{R} T_e)^{1/2}. \tag{3.15}$$

Rewriting the right-hand side of (3.11) as

$$\frac{k}{\rho_e T_e}\frac{\partial^2 T'}{\partial x^2} = \frac{k}{\rho_e}\left[\frac{\partial^2}{\partial x^2}\left(\frac{T'}{T_e}\right) + \frac{2}{T_e}\frac{\mathrm{d}T_e}{\mathrm{d}x}\frac{\partial}{\partial x}\left(\frac{T'}{T_e}\right) + \frac{1}{T_e}\frac{\mathrm{d}^2 T_e}{\mathrm{d}x^2}\frac{T'}{T_e}\right], \tag{3.16}$$

we neglect the second and third terms in the square brackets. While the neglect of the third term is legitimate by assumption, the second term may also be neglected because it is multiplied by the temperature gradient and smaller by χ than the first term, and also because the entropy change is evaluated only at the lowest order. Using (3.13) and (3.14) with S'/c_v neglected, the right-hand side of (3.11) may be approximated as

$$\frac{k}{\rho_e T_e}\frac{\partial^2 T'}{\partial x^2} = \frac{(\gamma-1)k}{\rho_e}\frac{\partial^2}{\partial x^2}\left(\frac{\rho'}{\rho_e}\right) = -\frac{(\gamma-1)k}{\gamma p_0}\frac{\partial^2 u}{\partial x \partial t}, \tag{3.17}$$

where the derivative of a_e with respect to x is dropped, consistent with the approximation that the temperature gradient has already been neglected in (3.17). Thus the diffusive part of the entropy change can be evaluated just as in the case without the temperature gradient as follows:

$$\frac{\partial S_d'}{\partial x} = -\frac{(\gamma-1)k}{\gamma p_0}\frac{\partial^2 u}{\partial x^2}. \tag{3.18}$$

The small entropy change affects (3.5) through the pressure gradient, which is calculated by using (3.8) as

$$\frac{\partial p}{\partial x} = \frac{\partial p}{\partial \rho}\frac{\partial \rho}{\partial x} + \frac{\partial p}{\partial \rho_e}\frac{\mathrm{d}\rho_e}{\mathrm{d}x} + \frac{\partial p}{\partial S}\frac{\partial S}{\partial x} + \frac{\partial p}{\partial S_e}\frac{\mathrm{d}S_e}{\mathrm{d}x}, \tag{3.19}$$

where p is regarded as a function not only of ρ and S but also of x through ρ_e and S_e. But the last term cancels out the second term owing to (2.13). Hence the pressure gradient in (3.5) can be evaluated as

$$-\frac{1}{\rho}\frac{\partial p}{\partial x} = -\frac{\gamma p}{\rho}\left(\frac{1}{\rho}\frac{\partial \rho}{\partial x} - \frac{1}{\rho_e}\frac{\mathrm{d}\rho_e}{\mathrm{d}x}\right) - \frac{p}{c_v \rho}\left(\frac{\partial S}{\partial x} - \frac{\mathrm{d}S_e}{\mathrm{d}x}\right), \tag{3.20}$$

where the entropy change is given by

$$-\frac{p}{c_v \rho}\frac{\partial S'}{\partial x} = -\frac{p_0}{c_v \rho_e}\frac{\partial S_c'}{\partial x} + \frac{(\gamma-1)k}{c_p \rho_e}\frac{\partial^2 u}{\partial x^2}. \tag{3.21}$$

In the remainder of the treatment of the acoustic main flow, we follow a similar

procedure to that used previously by expressing the density in terms of the local adiabatic sound speed a defined by

$$a = \left(\frac{\partial p}{\partial \rho}\Big|_{S=S_e,x} \right)^{1/2} = a_e \left(\frac{\rho}{\rho_e} \right)^{(\gamma-1)/2}. \tag{3.22}$$

Using

$$\frac{1}{a_e}\frac{\mathrm{d}a_e}{\mathrm{d}x} = -\frac{1}{2\rho_e}\frac{\mathrm{d}\rho_e}{\mathrm{d}x} = \frac{1}{2T_e}\frac{\mathrm{d}T_e}{\mathrm{d}x}, \tag{3.23}$$

it follows from (3.4) and (3.5) that

$$\left[\frac{\partial}{\partial t} + (u \pm a)\frac{\partial}{\partial x}\right]\left[u \pm \frac{2}{\gamma-1}(a-a_e)\right] = \frac{2}{\gamma-1}\left[(a-a_e)a \pm (\gamma a - a_e)u\right]\left(\frac{1}{a_e}\frac{\mathrm{d}a_e}{\mathrm{d}x}\right) - \frac{p_0}{c_v\rho_e}\frac{\partial S_c'}{\partial x} \pm \frac{a}{A}\oint v_n \mathrm{d}s + v_{de}\frac{\partial^2 u}{\partial x^2}, \tag{3.24}$$

with the signs vertically ordered, where v_{de} denotes the diffusivity of sound defined by $v_e[4/3 + \mu_v/\mu + (\gamma-1)/Pr]$, v_e being the kinematical viscosity μ/ρ_e. Here note that v_e and v_{de} are functions of x determined by ρ_e. Equations (3.24) are supplemented by (3.10), which is rewritten, for later use, in terms of the gradient of a_e as

$$\frac{\partial S_c'}{\partial t} + \frac{2c_p}{a_e}\frac{\mathrm{d}a_e}{\mathrm{d}x}u = 0. \tag{3.25}$$

Thus (3.24) with (3.25) are closed for u and a by relating v_n to the quantities in the main flow.

4. Treatment of the boundary layer and the resonators

This section is devoted to evaluation of v_n. We first derive the expression for v_b given by (1.1) and then that due to the resonator.

4.1. *Linear theory of the boundary layer*

Since v_b is assumed to be small, the boundary layer is treated within the linear theory. The physical quantities in the boundary layer are assumed to be perturbed slightly from the local equilibrium values. Let the density, pressure, temperature, entropy, axial velocity and the velocity inward normal to the tube wall be represented, respectively, by $\rho_e+\tilde{\rho}$, $p_0+\tilde{p}$, $T_e+\tilde{T}$, $S_e+\tilde{S}$, $\tilde{u}$ and $\tilde{v}$. The quantities with tilde are regarded as being small and dependent not only on x and t but also on n, where n denotes the boundary-layer coordinate taken inward normal to the tube wall at $n = 0$. Substitution of these into the basic equations (2.1) to (2.3), and linearization about the local equilibrium state lead to

$$\frac{\partial \tilde{\rho}}{\partial t} + \frac{\partial}{\partial x}(\rho_e\tilde{u}) + \frac{\partial}{\partial n}(\rho_e\tilde{v}) = 0, \tag{4.1}$$

$$\rho_e\frac{\partial \tilde{u}}{\partial t} = -\frac{\partial \tilde{p}}{\partial x} + \mu\frac{\partial^2 \tilde{u}}{\partial n^2}, \tag{4.2}$$

$$0 = -\frac{\partial \tilde{p}}{\partial n}, \tag{4.3}$$

$$\rho_e T_e\left(\frac{\partial \tilde{S}}{\partial t} + \tilde{u}\frac{\mathrm{d}S_e}{\mathrm{d}x}\right) = k\frac{\partial^2 \tilde{T}}{\partial n^2}, \tag{4.4}$$

where the boundary-layer approximation has been used. The non-slip and isothermal boundary conditions are imposed on the tube wall as

$$\tilde{u} = \tilde{v} = 0 \quad \text{and} \quad \tilde{T} = 0 \quad \text{at } n = 0. \tag{4.5}$$

On the other hand, as the edge of the boundary layer is approached, i.e. $n \to \infty$, the physical quantities should match with those in the acoustic main flow:

$$\lim_{n\to\infty} [\rho_e + \tilde{\rho},\ p_0 + \tilde{p},\ T_e + \tilde{T},\ S_e + \tilde{S},\ \tilde{u},\ \tilde{v}] = [\rho,\ p,\ T,\ S,\ u,\ v_b]. \tag{4.6}$$

Here the quantities on the right-hand side of (4.6) satisfy (3.4) to (3.8), but their linearized relations are sufficient for the treatment of the linear boundary layer.

So far we have not referred to (3.4), which is now linearized as

$$\frac{\partial}{\partial t}\left(\frac{\rho'}{\rho_e}\right) + \frac{\partial u}{\partial x} + \frac{1}{\rho_e}\frac{\mathrm{d}\rho_e}{\mathrm{d}x}u = 0. \tag{4.7}$$

Here the right-hand side of (3.4) is much smaller and has been neglected. Using $\rho'/\rho_e = p'/\rho_e a_e^2 - S'/c_p$ derived from the first relation of (3.13), and (3.10) with $S_c' \approx S'$ to replace the first term of (4.7), it is reduced to the same equation as for the adiabatic process in the case without the temperature gradient:

$$\frac{1}{\rho_e a_e^2}\frac{\partial p'}{\partial t} + \frac{\partial u}{\partial x} = 0 \quad \text{or} \quad \frac{\partial}{\partial t}\left(\frac{p'}{p_0}\right) + \gamma\frac{\partial u}{\partial x} = 0. \tag{4.8}$$

Equation (4.8) is also expressed in terms of T' by using $p'/p_0 = \gamma(T'/T_e - S'/c_p)/(\gamma - 1)$ derived from (3.13), and (3.10) as

$$\frac{\partial}{\partial t}\left(\frac{T'}{T_e}\right) + (\gamma - 1)\frac{\partial u}{\partial x} + \frac{1}{T_e}\frac{\mathrm{d}T_e}{\mathrm{d}x}u = 0. \tag{4.9}$$

Elimination of p' or u in (4.8) and (3.14) leads to the linear, lossless wave equations with a temperature gradient:

$$\frac{\partial^2 u}{\partial t^2} = a_e^2\frac{\partial^2 u}{\partial x^2} \quad \text{or} \quad \frac{\partial^2 p'}{\partial t^2} = \frac{\partial}{\partial x}\left(a_e^2\frac{\partial p'}{\partial x}\right). \tag{4.10}$$

In view of the matching condition (4.6), we seek the boundary-layer solutions by making the following replacement of the variables:

$$[\rho_e + \tilde{\rho},\ p_0 + \tilde{p},\ T_e + \tilde{T},\ S_e + \tilde{S},\ \tilde{u},\ \tilde{v}] = [\rho + \breve{\rho},\ p + \breve{p},\ T + \breve{T},\ S + \breve{S},\ u + \breve{u},\ \breve{v}], \tag{4.11}$$

where the quantities with breve depend on n as well as x and t. Note the difference between the quantities designated by a prime, tilde and breve. The quantities with a prime and tilde represent, respectively, the small deviations in the main flow and in the boundary layer from the local equilibrium state. The quantities with a breve are introduced only for the sake of convenience of mathematical treatment and the following relation holds except for $\tilde{v}$ and $\breve{v}$: $\tilde{(\ )} = (\ )' + \breve{(\ )}$. Substituting the replacement (4.11) in (4.1), (4.2) and (4.4), and using the linearized relations for the acoustic main flow, we have

$$\frac{\partial \breve{\rho}}{\partial t} + \frac{\partial}{\partial x}(\rho_e \breve{u}) + \frac{\partial}{\partial n}(\rho_e \breve{v}) = 0, \tag{4.12}$$

$$\frac{\partial \breve{u}}{\partial t} = -\frac{1}{\rho_e}\frac{\partial \breve{p}}{\partial x} + \frac{\mu}{\rho_e}\frac{\partial^2 \breve{u}}{\partial n^2}, \tag{4.13}$$

$$\frac{\partial \check{S}}{\partial t} + \check{u}\frac{\mathrm{d}S_e}{\mathrm{d}x} = \frac{k}{\rho_e T_e}\frac{\partial^2 \check{T}}{\partial n^2}. \tag{4.14}$$

The boundary-layer approximation suggests that the pressure in the main flow prevails into the boundary layer so that $\check{p}$ vanishes identically. Using this and the equation of state (3.7), we obtain

$$\frac{\check{\rho}}{\rho_e} + \frac{\check{T}}{T_e} = 0, \tag{4.15}$$

where the linearized version of (3.7) for the main flow has been used. From (3.8), similarly, $\check{S}$ is derived as follows:

$$\check{S} = -\frac{c_p \check{\rho}}{\rho_e} = \frac{c_p \check{T}}{T_e}. \tag{4.16}$$

Using $\check{p} \equiv 0$, (4.13) and (4.14) with (3.12) are reduced to the following equations:

$$\frac{\partial \check{u}}{\partial t} = \nu_e \frac{\partial^2 \check{u}}{\partial n^2}, \tag{4.17}$$

and

$$\frac{\partial \check{T}}{\partial t} + \check{u}\frac{\mathrm{d}T_e}{\mathrm{d}x} = \frac{\nu_e}{Pr}\frac{\partial^2 \check{T}}{\partial n^2}, \tag{4.18}$$

where ν_e/Pr $(= k/\rho_e c_p)$ is the thermal diffusivity and Pr is assumed constant. By (4.11), the boundary conditions (4.5) and the matching conditions (4.6) are imposed as follows:

$$\check{u} = -u \quad \text{and} \quad \check{T} = -T + T_e \quad \text{at } n = 0, \tag{4.19}$$

and

$$\check{u} \to 0 \quad \text{and} \quad \check{T} \to 0 \quad \text{as } n \to \infty. \tag{4.20}$$

Equations (4.17) and (4.18) are easily solvable by taking the Fourier transform with respect to t. When $\check{u}$ and $\check{T}$ are obtained, the velocity at the edge of the boundary layer, denoted by v_b, is obtained by integrating (4.12) from the wall to the edge of the boundary layer at $n = \infty$ as

$$v_b = \int_0^\infty \frac{\partial \check{v}}{\partial n}\mathrm{d}n = \int_0^\infty \left[\frac{\partial}{\partial t}\left(\frac{\check{T}}{T_e}\right) - \frac{\partial \check{u}}{\partial x} + \frac{1}{T_e}\frac{\mathrm{d}T_e}{\mathrm{d}x}\check{u}\right]\mathrm{d}n, \tag{4.21}$$

where (4.15) and (3.12) have been used. Carrying out this integration (see Appendix A), v_b is obtained in terms of u as

$$v_b = \left(1 + \frac{\gamma - 1}{\sqrt{Pr}}\right)\sqrt{\nu_e}\frac{\partial^{-1/2}}{\partial t^{-1/2}}\left(\frac{\partial u}{\partial x}\right) + \left(\frac{1}{2} + \frac{1}{\sqrt{Pr} + Pr}\right)\frac{\sqrt{\nu_e}}{T_e}\frac{\mathrm{d}T_e}{\mathrm{d}x}\frac{\partial^{-1/2}u}{\partial t^{-1/2}}. \tag{4.22}$$

This is the basic relation to associate the boundary layer with the main flow. The first term on the right-hand side is due to the ordinary wall friction while the second term is due to the temperature gradient. Both are expressed in terms of the derivative of $-1/2$-order with respect to t but the first term is that of $\partial u/\partial x$ whereas the second one is that of u itself. Hence note that the hereditary effects appear differently. Using (4.8) to eliminate $\partial u/\partial x$, v_b is expressed in the mixed form of p' and u as in (1.1). Note also that expression (4.22), in the context of the linear theory of the boundary layer, is valid even when the temperature gradient is not necessarily small, i.e. $\chi \approx 1$.

Finally the heat flux Q_n through the wall into the boundary layer can also be

calculated by

$$Q_n = -k\frac{\partial}{\partial n}(T_e + \tilde{T})\Big|_{n=0} = -k\frac{\partial \check{T}}{\partial n}\Big|_{n=0}. \tag{4.23}$$

This is given by

$$Q_n = k\sqrt{\frac{Pr}{\nu_e}}\left[(\gamma-1)T_e\frac{\partial^{-1/2}}{\partial t^{-1/2}}\left(\frac{\partial u}{\partial x}\right) + \frac{1}{1+\sqrt{Pr}}\frac{\mathrm{d}T_e}{\mathrm{d}x}\frac{\partial^{-1/2}u}{\partial t^{-1/2}}\right], \tag{4.24}$$

in terms of u or alternatively by

$$Q_n = -k\sqrt{\frac{Pr}{\nu_e}}\left(\frac{\partial^{1/2}T}{\partial t^{1/2}} + \frac{\sqrt{Pr}}{1+\sqrt{Pr}}\frac{\mathrm{d}T_e}{\mathrm{d}x}\frac{\partial^{-1/2}u}{\partial t^{-1/2}}\right), \tag{4.25}$$

in terms of the mixed form of T and u (see Appendix A), where $k\sqrt{Pr/\nu_e} = \sqrt{kc_p\rho_e}$. Because $\sqrt{\nu_e}$ is proportional to $\sqrt{T_e}$, the first term (4.24) (with the factor outside the brackets) is proportional to $\sqrt{T_e}$ while the second term is proportional to $1/\sqrt{T_e}$. Comparing (4.24) with (4.22), it is found that the first and second terms in the respective equations agree with each other in the power of T_e. Although the respective sums of the first and second terms in v_b and Q_n are not proportional to each other, even ignoring the dimensions, we will find that v_b is directed almost in the same sense as Q_n. Here note that because the n component of the heat-flux vector vanishes at the edge of the boundary layer, the heat flux does not enter the main-flow region but is in the boundary layer along the wall.

4.2. *Linear theory of Helmholtz resonators*

Because the treatment of the Helmholtz resonator is given in a previous paper (Sugimoto 1992), we only summarize the essential results. The resonator consists of a bulbous cavity and a straight throat. The cavity shape may be arbitrary and the throat cross-section may also be of arbitrary shape but uniform along its axis. The cavity volume V is much larger than the throat volume BL, B and L being, respectively, the cross-sectional area of the throat and its axial length.

For the gas in the cavity, no account of its motion is taken and only conservation of mass is considered:

$$V\frac{\partial \rho_c}{\partial t} = Bq, \tag{4.26}$$

where ρ_c and q denote, respectively, the mean density of the gas in the cavity and the mean mass flux density into the cavity, which is averaged over the whole cross-section of the throat. For the gas in the throat, no account of compressibility is taken because a typical wavelength is assumed much longer than the throat length. This implies that q is uniform in the axial direction of the throat. Noting this and that q also represents the momentum density, the momentum balance of all the gas contained in the throat yields

$$L\frac{\partial q}{\partial t} = -p_c + p - F_r, \tag{4.27}$$

where p is the pressure at the orifice on the tube side and F_r is the total friction force on the throat wall. This force is given by

$$F_r = \frac{2\rho_e\sqrt{\nu_e}L}{r}\frac{\partial^{1/2}w}{\partial t^{1/2}}, \tag{4.28}$$

where r and w denote, respectively, the hydraulic radius of the throat (not to be

confused with r for the radial coordinate used only in § 2) and the mean velocity of gas averaged over the whole cross-section of the throat. Note that w is uniform along the throat.

Because we are concerned with the linear theory, it follows from (4.26) that

$$q = \rho_e w = \frac{V}{B}\frac{\partial \rho_c'}{\partial t} = \frac{V}{Ba_e^2}\frac{\partial p_c'}{\partial t}, \tag{4.29}$$

where ρ_c' $(= \rho_c - \rho_e)$ and p_c' $(= p_c - p_0)$ are, respectively, the excess density and pressure in the cavity, and the lowest relation $p_c' = a_e^2 \rho_c'$ has been used. Eliminating q between (4.26) and (4.27), and using (4.28) and (4.29), we derive

$$\frac{\partial^2 p_c'}{\partial t^2} + \frac{2\nu_e^{1/2}}{r}\frac{\partial^{3/2} p_c'}{\partial t^{3/2}} + \omega_e^2 p_c' = \omega_e^2 p', \tag{4.30}$$

where ω_e $(= \sqrt{Ba_e^2/LV})$ is the natural angular frequency of the resonator and the derivative of 3/2-order is defined by differentiating the one of 1/2-order once with respect to t. Note that since a_e depends on x, ω_e varies with x. End corrections to the throat are ignored here for simplicity (see Sugimoto 1992).

4.3. *Evaluation of the integral*

With v_b and w thus specified, we can now evaluate the integral in (3.24). For treatment of the array of resonators, we suppose that identical resonators are connected to the tube with equal axial spacing d, which is assumed to be much smaller than a typical wavelength in the tube. Each resonator is assumed to be small in the sense that the cavity volume is much smaller than the tube volume per spacing. This is measured by a small parameter κ defined by

$$\kappa = \frac{V}{Ad} \ll 1. \tag{4.31}$$

These assumptions enable us to make a continuum approximation for a discrete distribution of resonators, namely to average the integral in (3.24) per unit axial length of x as

$$\frac{1}{A}\oint v_b \mathrm{d}s = \frac{1}{A}\left[\left(\frac{2A}{R} - NB\right)v_b - NBw\right], \tag{4.32}$$

where R is the hydraulic radius of the tube and N $(= 1/d)$ is the number density of resonators per unit axial length. Substituting v_b and w given, respectively, by (4.22) and (4.29) into the right-hand side of (4.32), it follows that

$$\frac{1}{A}\oint v_n \mathrm{d}s = \frac{2\sqrt{\nu_e}}{R^*}\left[C\frac{\partial^{-1/2}}{\partial t^{-1/2}}\left(\frac{\partial u}{\partial x}\right) + \frac{C_T}{T_e}\frac{\mathrm{d}T_e}{\mathrm{d}x}\frac{\partial^{-1/2} u}{\partial t^{-1/2}}\right] - \frac{\kappa}{\gamma p_0}\frac{\partial p_c'}{\partial t}, \tag{4.33}$$

with $1/R^* = (1 - NBR/2A)/R$ where R^* is called the reduced radius of the tube, and C and C_T are defined, respectively, as

$$C = 1 + \frac{\gamma - 1}{\sqrt{Pr}}, \quad C_T = \frac{1}{2} + \frac{1}{\sqrt{Pr} + Pr}. \tag{4.34}$$

5. Nonlinear wave equations

5.1. *Derivation of the equations for unidirectional propagation*

We now proceed to derive from (3.24) the equations describing unidirectional propagation in the positive direction of x. We again remark that the right-hand sides are

small quantities since they are due to the effects of viscosity, heat conduction and the temperature gradient as well as the small effect of the resonators. If they are all ignored, then the wave propagation is governed by the left-hand sides. It then follows that

$$u \pm \frac{2}{\gamma - 1}(a - a_e) = C^{\pm} \quad \text{along the characteristics} \quad \frac{\mathrm{d}x}{\mathrm{d}t} = u \pm a, \tag{5.1}$$

with the signs vertically ordered, where $C^{\pm}$ are well-known Riemann invariants. Assuming an equilibrium state far ahead of propagation, we have a simple wave in which one of the characteristics, C^{-}, is taken to vanish so that

$$u = \frac{2}{\gamma - 1}(a - a_e). \tag{5.2}$$

In accordance with this, the following relations hold among the other variables within the same approximation:

$$\frac{u}{a_e} = \frac{2}{\gamma - 1}\left(\frac{a - a_e}{a_e}\right) = \frac{\rho_e - \rho}{\rho_e} = \frac{p - p_0}{\gamma p_0} = \frac{1}{\gamma - 1}\left(\frac{T - T_e}{T_e}\right). \tag{5.3}$$

These are simply the adiabatic relations which ignore the effect of the temperature gradient. Using (5.2) and only taking account of linear terms on the right-hand side of (3.24) with the upper sign, we can derive the equation for u which includes the small effects on the right-hand side as

$$\frac{\partial}{\partial t}\left[\frac{\partial u}{\partial t} + \left(a_e + \frac{\gamma + 1}{2}u\right)\frac{\partial u}{\partial x}\right] = \frac{\partial}{\partial t}\left(\frac{3}{2}u\frac{\mathrm{d}a_e}{\mathrm{d}x}\right) + \frac{\partial}{\partial x}\left(ua_e\frac{\mathrm{d}a_e}{\mathrm{d}x}\right) + \frac{a_e}{2A}\frac{\partial}{\partial t}\oint v_n \mathrm{d}s + \frac{\nu_{de}}{2}\frac{\partial^3 u}{\partial t \partial x^2}, \tag{5.4}$$

where S_c' has been eliminated by differentiating (3.24) with respect to t to use (3.25).

In order to focus on behaviour in the far field, we introduce a retarded time θ in a frame moving with a local sound speed and a far-field coordinate X associated with the nonlinearity ε, which are defined, respectively, by

$$\theta = \omega\left(t - \int_0^x \frac{\mathrm{d}x}{a_e}\right), \quad X = \varepsilon\omega\int_0^x \frac{\mathrm{d}x}{a_e}. \tag{5.5}$$

By this transformation, the differential operators $\partial/\partial t$ and $\partial/\partial x$ are replaced, respectively, by

$$\frac{\partial}{\partial t} = \omega\frac{\partial}{\partial \theta}, \quad \frac{\partial}{\partial x} = -\frac{\omega}{a_e}\frac{\partial}{\partial \theta} + \varepsilon\frac{\omega}{a_e}\frac{\partial}{\partial X}. \tag{5.6}$$

Then (5.4) is rewritten after integrated with respect to θ as

$$\frac{\varepsilon}{a_e}\frac{\partial u}{\partial X} - \frac{\gamma + 1}{2}\frac{u}{a_e^2}\frac{\partial u}{\partial \theta} = \frac{\varepsilon}{2a_e^2}\frac{\mathrm{d}a_e}{\mathrm{d}X}u + \frac{1}{2\omega A}\oint v_n \mathrm{d}s + \frac{\nu_{de}\omega}{2a_e^3}\frac{\partial^2 u}{\partial \theta^2}, \tag{5.7}$$

where only the lowest-order terms among small quantities have been retained and an integration constant dependent on X has been set equal to zero because of the undisturbed state as $\theta \to -\infty$ (i.e. $x \to \infty$).

Here we should make the following point. So far T_e has been regarded formally as a function of X. But the mild dependence of T_e on X has now to be considered. Since T_e varies over the axial distance l, the original argument of T_e is taken to be

x/l. Therefore T_e depends on X through the argument $\chi X/\varepsilon$. Thus the temperature gradient is taken to be

$$\frac{1}{T_e}\frac{\mathrm{d}T_e}{\mathrm{d}X} = \frac{\chi}{\varepsilon}\frac{\dot{H}_e}{H_e} \quad \text{with} \quad H_e = \frac{T_e}{T_0}, \tag{5.8}$$

with $T_0 = T_e$ at $X = 0$ where the dot over T_e designates differentiation with respect to the argument $\chi X/\varepsilon$ and $\dot{H}_e/H_e$ is regarded as a quantity of order unity. In the following, we assume that $\varepsilon \ll \chi$.

To make u in (5.7) and p_c' in (4.30) dimensionless, we set

$$\varepsilon f \equiv \frac{(\gamma+1)}{2}\frac{u}{a_e}\left(\approx \frac{(\gamma+1)}{2\gamma}\frac{p'}{p_0}\right), \quad \varepsilon g \equiv \frac{(\gamma+1)}{2\gamma}\frac{p_c'}{p_0}, \tag{5.9}$$

where f and g are assumed to be order of unity. By using these, it follows from (5.7) that

$$\frac{\partial f}{\partial X} - f\frac{\partial f}{\partial \theta} + \frac{1}{4H_e}\frac{\mathrm{d}H_e}{\mathrm{d}X}f = -\delta_e\frac{\partial^{1/2} f}{\partial \theta^{1/2}} + \frac{\lambda_e}{H_e}\frac{\mathrm{d}H_e}{\mathrm{d}X}\frac{\partial^{-1/2} f}{\partial \theta^{-1/2}} + \beta\frac{\partial^2 f}{\partial \theta^2} - K\frac{\partial g}{\partial \theta}, \tag{5.10}$$

and from (4.30) that

$$\frac{\partial^2 g}{\partial \theta^2} + \delta_{re}\frac{\partial^{3/2} g}{\partial \theta^{3/2}} + \Omega_e g = \Omega_e f, \tag{5.11}$$

where the coefficients are defined as

$$\left.\begin{aligned} \delta_e = C\frac{\sqrt{v_e/\omega}}{\varepsilon R^*}, \quad \lambda_e = \left(\frac{C}{4} + C_T\right)\frac{\sqrt{v_e/\omega}}{R^*}, \quad \beta = \frac{v_{de}\omega}{2\varepsilon a_e^2}, \\ K = \frac{\kappa}{2\varepsilon}, \quad \delta_{re} = \frac{2\sqrt{v_e/\omega}}{r}, \quad \Omega_e = \left(\frac{\omega_e}{\omega}\right)^2 \end{aligned}\right\}. \tag{5.12}$$

These are the equations which include all the effects of nonlinearity, dissipation and the array of resonators. The first two terms on the left-hand side of (5.10) represent the spatial evolution of nonlinear acoustic waves propagating unidirectionally and the third term represents the lossless effect due to the non-uniform equilibrium state with the temperature gradient. Because of the assumption $\varepsilon \ll \chi$ and (5.8), the third term dominates the second one so that the first term balances with the third one to the lowest approximation, i.e. $\partial f/\partial X + (f/4H_e)\mathrm{d}H_e/\mathrm{d}X \approx 0$. This relation may be derived directly from the first equation of (4.10) for u by introducing the transformation (5.5).

On the other hand, the first and second terms on the right-hand side result from v_b and represent the effects due to the boundary layer. They are proportional to the ratio of a typical thickness of the boundary layer $\sqrt{v_e/\omega}$ to the reduced radius R^*, and are expressed in terms of the derivatives of $+1/2$- and $-1/2$-order, respectively. The third term is responsible for the diffusive effect inherent to the acoustic waves. Although β appears to depend on x, it is independent of x because $v_e/a_e^2 = \mu/\gamma p_0$ and therefore the subscript e is dropped. The value of β is found to be extremely small and negligible unless a shock structure is concerned. The last term is due to the array of resonators and is the same as in the case without the temperature gradient. For the response of the resonators, (5.11) is the same except that the coefficients depend on T_e.

By the normalization above, v_b is expressed in terms of f as

$$v_b = \frac{2\varepsilon^2\omega R^*}{\gamma+1}\left(-\delta_e\frac{\partial^{1/2} f}{\partial \theta^{1/2}} + \frac{\lambda_e}{H_e}\frac{\mathrm{d}H_e}{\mathrm{d}X}\frac{\partial^{-1/2} f}{\partial \theta^{-1/2}}\right), \tag{5.13}$$

where the lowest-order relation $\partial f/\partial X+(f/4H_e)\mathrm{d}H_e/\mathrm{d}X \approx 0$ has been used to replace the term $\partial f/\partial X$ resulting from $\partial u/\partial x$ in (4.22). If the assumption $\varepsilon \ll \chi$ is removed and the case with $\chi \approx \varepsilon$ is considered, the full lossless version of (5.10) is employed to evaluate $\partial f/\partial X$. Then the first term on the right-hand side of (5.10) includes additional terms accordingly. In a similar way to above, Q_n is expressed as

$$Q_n = \frac{2\varepsilon^2\omega c_p\rho_e T_e R^*}{\gamma+1}\left[-\left(\frac{C-1}{C}\right)\delta_e\frac{\partial^{1/2}f}{\partial\theta^{1/2}}+\left(\frac{C+4C_T-3}{C+4C_T}\right)\frac{\lambda_e}{H_e}\frac{\mathrm{d}H_e}{\mathrm{d}X}\frac{\partial^{-1/2}f}{\partial\theta^{-1/2}}\right], \tag{5.14}$$

where $2\varepsilon^2\omega c_p\rho_e T_e R^*/(\gamma+1) = 2\varepsilon^2\gamma\omega p_0 R^*/(\gamma^2-1)$.

5.2. *Properties of the equations*

Here we examine some solutions to (5.10) and (5.11) in simplified cases and discuss the properties derived from the equations. If all dissipative effects are ignored, they are reduced, respectively, to

$$\frac{\partial f}{\partial X}-f\frac{\partial f}{\partial\theta}+\frac{1}{4H_e}\frac{\mathrm{d}H_e}{\mathrm{d}X}f = -K\frac{\partial g}{\partial\theta}, \tag{5.15}$$

and

$$\frac{\partial^2 g}{\partial\theta^2}+\Omega_e g = \Omega_e f. \tag{5.16}$$

Further, if the array of resonators is absent, i.e. $K = 0$, (5.15) describes lossless propagation under the temperature gradient. Then the solution is easily found as

$$\frac{\mathrm{d}f}{\mathrm{d}X} = -\frac{1}{4H_e}\frac{\mathrm{d}H_e}{\mathrm{d}X}f \quad \text{along a characteristic curve} \quad \frac{\mathrm{d}\theta}{\mathrm{d}X} = -f. \tag{5.17}$$

Along this, f varies as

$$f = H_e^{-1/4}F(\xi), \tag{5.18}$$

with $H_e(0) = 1$ where ξ is a parameter specifying the characteristic curve, which starts from $\theta = \xi$ at $X = 0$, and $F(\xi)$ is the initial value of f at $X = 0$ and $\theta = \xi$. Using (5.18), the characteristic curve is expressed as

$$\theta = -F(\xi)\int_0^X H_e^{-1/4}\mathrm{d}X+\xi. \tag{5.19}$$

Elimination of the parameter ξ gives the solution for f.

It is found from (5.18) and (5.9) that as the temperature is increased toward the direction of propagation, the pressure p' decreases as $H_e^{-1/4}$ whereas the velocity u increases as $H_e^{1/4}$ because a_e is proportional to $H_e^{1/2}$. When the temperature is decreased, the reverse holds. Note that p' and u behave oppositely so that the energy flux (intensity) $p'u$ does not change. The 1/4 power law is the consequence of the approximation of the geometrical acoustics (Pierce 1991), in which variations of the non-uniform equilibrium state due to the temperature gradient are assumed to be mild over the typical wavelength ($\chi \ll 1$). Because the power 1/4 is mild, a strong, small compression pulse ($f > 0$) imposed initially will evolve into a shock eventually. This will be formed at a position given by the least positive solution of X which satisfies the equation

$$-\frac{\mathrm{d}F}{\mathrm{d}\xi}\int_0^X H_e^{-1/4}\mathrm{d}X+1 = 0. \tag{5.20}$$

Suppose that the shock is formed when the temperature gradient is absent, i.e. $H_e = 1$. If the positive temperature gradient is imposed so that $H_e > 1$ for $X > 0$, then the shock is formed at a position of X further down than the one in the case without the gradient. On the contrary, if the negative gradient is imposed so that $H_e < 1$ for $X > 0$, then it is formed at a position closer to $X = 0$.

When the array is connected, a solution is not so easily available. In general, however, it is easily shown by multiplying (5.15) by $H_e^{1/4}$ and integrating over the whole domain of θ that the following conservation holds with respect to X:

$$\frac{\mathrm{d}I_1}{\mathrm{d}X} = 0 \quad \text{with} \quad I_1(X) = \int_{-\infty}^{\infty} H_e^{1/4} f \mathrm{d}\theta, \tag{5.21}$$

where f and g are assumed to vanish at both infinities of θ. The conserved quantity I_1 possesses no physical meaning. The first-order quantity in f is the mass flux $\rho_e u$, and is given by $H_e^{-1/2} f$ except for a numerical factor. But the power of H_e is different. Conversely, the mass flux is not conserved. There is another conserved quantity. As is expected from the result of the geometrical acoustics, the total energy flux $p'u$ which passes at some position X from $\theta = -\infty$ to ∞ is conserved with respect to X. In fact, since $p'u \propto (a_e/a_0) f^2 \propto H_e^{1/2} f^2$ by use of the relation (5.9), it follows on multiplying (5.15) by $H_e^{1/2} f$ and integrating it over θ that

$$\frac{\mathrm{d}I_2}{\mathrm{d}X} = 0 \quad \text{with} \quad I_2(X) = \int_{-\infty}^{\infty} H_e^{1/2} f^2 \mathrm{d}\theta, \tag{5.22}$$

where f is assumed to vanish at both infinities of θ. This equality results from the integral

$$-K H_e^{1/2} \int_{-\infty}^{\infty} f \frac{\partial g}{\partial \theta} \mathrm{d}\theta = -K H_e^{1/2} \left[\frac{1}{2\Omega_e} \left(\frac{\partial g}{\partial \theta} \right)^2 + \tfrac{1}{2} g^2 \right]_{\theta=-\infty}^{\theta=\infty} = 0, \tag{5.23}$$

where (5.16) has been used and both g and $\partial g/\partial \theta$ are assumed to vanish as $|\theta| \to \infty$. In view of (5.22), it is interesting to note that the energy flux cannot be amplified without recourse to the dissipative effects usually leading to its attenuation.

So we consider the full equations (5.10) and (5.11). Following the same method that leads to (5.21) and (5.22), we obtain, respectively,

$$\frac{\mathrm{d}I_1}{\mathrm{d}X} = H_e^{1/4} \int_{-\infty}^{\infty} \left(-\delta_e \frac{\partial^{1/2} f}{\partial \theta^{1/2}} + \frac{\lambda_e}{H_e} \frac{\mathrm{d}H_e}{\mathrm{d}X} \frac{\partial^{-1/2} f}{\partial \theta^{-1/2}} \right) \mathrm{d}\theta, \tag{5.24}$$

and

$$\frac{\mathrm{d}I_2}{\mathrm{d}X} = 2H_e^{1/2} \int_{-\infty}^{\infty} \left[\left(-\delta_e \frac{\partial^{1/2} f}{\partial \theta^{1/2}} + \frac{\lambda_e}{H_e} \frac{\mathrm{d}H_e}{\mathrm{d}X} \frac{\partial^{-1/2} f}{\partial \theta^{-1/2}} \right) f - \beta \left(\frac{\partial f}{\partial \theta} \right)^2 - \frac{\delta_{re} K}{\Omega_e} \frac{\partial g}{\partial \theta} \frac{\partial^{3/2} g}{\partial \theta^{3/2}} \right] \mathrm{d}\theta, \tag{5.25}$$

where f, $\partial f/\partial \theta$, g and $\partial g/\partial \theta \to 0$ as $|\theta| \to \infty$, with the proviso that the integrals I_1 and I_2 exist. If so, I_1 and I_2 are no longer conserved with respect to X. In (5.25), the terms in the first parentheses on the right-hand side are proportional to v_b so that the product with f corresponds to the power input or output, depending on the sign. On the contrary, the term with β contributes obviously to decrease the energy flux. The last term results from the friction on the throat wall and physically decreases the

energy flux, although this is not straightforwardly seen from its form. By using the identity $\partial/\partial\theta(\partial^{-1/2}f/\partial\theta^{-1/2}) = \partial^{1/2}f/\partial\theta^{1/2}$ to integrate in part the first term on the right-hand side of (5.25), the terms on this side may be rewritten as

$$2H_e^{1/2}\int_{-\infty}^{\infty}\left[\left(\delta_e\frac{\partial f}{\partial\theta}+\frac{\lambda_e}{H_e}\frac{\mathrm{d}H_e}{\mathrm{d}X}f\right)\frac{\partial^{-1/2}f}{\partial\theta^{-1/2}}-\beta\left(\frac{\partial f}{\partial\theta}\right)^2-\frac{\delta_{re}K}{\Omega_e}\frac{\partial g}{\partial\theta}\frac{\partial^{3/2}g}{\partial\theta^{3/2}}\right]\mathrm{d}\theta. \tag{5.26}$$

When a compression pulse is imposed initially, f is positive everywhere. If f remains so in the course of propagation, the derivative of $-1/2$-order is always positive by definition. But the quantity $\partial f/\partial\theta$ necessarily changes its sign with respect to θ. Provided the integral (5.26) can be made positive by imposing the temperature gradient suitably, then the energy flux will be amplified against the intrinsic loss.

Using the definitions of δ_e and λ_e in (5.12), and (5.8), the quantities in the first parentheses of (5.26) are expressed as

$$\frac{\sqrt{\nu_e/\omega}}{\varepsilon R^*}\left[C\frac{\partial f}{\partial\theta}+\chi\left(\frac{C}{4}+C_T\right)\frac{\dot{H}_e}{H_e}f\right]. \tag{5.27}$$

Because the amplification as well as the damping occur by the same action of the boundary layer, the ratio of the typical thickness of the boundary layer $\sqrt{\nu_e/\omega}$ to the reduced radius R^* is commonly factored out of the brackets. In order to make the integral (5.26) positive, it is required at least that (5.27) should be made positive. But because $\partial f/\partial\theta$ changes sign, the possibility of amplification will depend delicately on the three values of f, $\partial f/\partial\theta$ and χ.

6. Evolution of compression pulses

We now proceed to solve an initial-value problem for (5.10) and (5.11) to examine whether or not the energy flux is amplified. First, we renormalize the equations by the following replacements to remove the parameters ε and ω used in the derivation of the equations but left unspecified quantitatively:

$$(f,\ g)\to(Kf,\ Kg)\quad\text{and}\quad(\theta,\ X)\to(\theta/\sqrt{\Omega_0},\ X/K\sqrt{\Omega_0}), \tag{6.1}$$

with $\Omega_0 = \Omega_e$ at $X = 0$. Then K and Ω_e in (5.10) and (5.11) may be set equal to unity and H_e, respectively, while θ and X are redefined, respectively, as

$$\theta=\omega_0\left(t-\int_0^x\frac{\mathrm{d}x}{a_e}\right),\quad X=\frac{\kappa\omega_0}{2}\int_0^x\frac{\mathrm{d}x}{a_e}, \tag{6.2}$$

with $\omega_0 = \omega_e$ at $X = 0$. The replacements (6.1) are equivalent to the choice that $\varepsilon = \kappa/2$ and $\omega = \omega_0$. The other parameters δ_e, λ_e, δ_{re} and β are transformed as

$$(\delta_e,\ \lambda_e,\ \delta_{re},\ \beta)\ \to\ (\delta_e/K\Omega_0^{1/4},\ \lambda_e/K\Omega_0^{1/4},\ \delta_{re}/\Omega_0^{1/4},\ \beta\Omega_0^{1/2}/K), \tag{6.3}$$

and the quantities on the right-hand side take the following values, respectively:

$$\left(\frac{2C\sqrt{\nu_e/\omega_0}}{\kappa R^*},\ \frac{(C+4C_T)\sqrt{\nu_e/\omega_0}}{4R^*},\ \frac{2\sqrt{\nu_e/\omega_0}}{r},\ \frac{\nu_{de}\omega_0}{\kappa a_e^2}\right). \tag{6.4}$$

Since ν_e increases as T_e, all the coefficients except for β are proportional to $\sqrt{H_e}$ as

$$(\delta_e,\ \lambda_e,\ \delta_{re}) = (\delta_0,\ \lambda_0,\ \delta_{r0})\sqrt{H_e}. \tag{6.5}$$

Here and hereafter the subscript 0 which replaces the subscript e designates the values of the respective quantities at $X = 0$. In the following, (5.10) and (5.11) with the variables and the coefficients thus redefined are solved.

The initial-value problem is posed as follows:

$$f(\theta,\ X = 0) = F(\theta) \quad \text{and} \quad g(\theta,\ X = 0) = G(\theta), \tag{6.6}$$

where $G(\theta)$ is imposed as a solution to (5.11) with f given by $F(\theta)$ and cannot be prescribed independently of F. The initial value F is limited to a compression pulse so that F is absolutely positive for any value of θ. One interesting choice of F is the acoustic-solitary-wave solution in the lossless case. Another choice is a smoothed square pulse. The reason for this choice lies in that $\partial f/\partial\theta$ vanishes in a plateau region of the pulse so that the condition for amplification is expected to be met easily.

For the temperature distribution, we assume that T_e increases linearly with respect to x as

$$\frac{T_e}{T_0} = 1 + \frac{x}{l}. \tag{6.7}$$

Then it follows that

$$\frac{a_e}{a_0} = \left(1 + \frac{x}{l}\right)^{1/2}. \tag{6.8}$$

According to the definition of X in (6.2), we have

$$X = \frac{\kappa\omega_0}{2}\int_0^x \frac{\mathrm{d}x}{a_e} = \frac{\kappa\omega_0 l}{a_0}\left[\left(1 + \frac{x}{l}\right)^{1/2} - 1\right]. \tag{6.9}$$

As a consequence, $H_e(= T_e/T_0)$ is expressed in terms of X as follows:

$$H_e = \left(1 + \frac{a_0}{\kappa\omega_0 l}X\right)^2. \tag{6.10}$$

Here we evaluate the coefficients δ_0, λ_0, δ_{r0} and β for tube used in our previous experiment without imposing the temperature gradient: $R = 0.04\,\mathrm{m}$ ($R^* = 0.0401\,\mathrm{m}$), $r = 0.00356\,\mathrm{m}$, $d = 0.05\,\mathrm{m}$, and $\kappa \approx 0.2$ (Sugimoto *et al.* 1999). Although there might be other tubes suitable for amplification, as a first attempt we shall start with this tube. For air at atmospheric pressure at room temperature 15° as reference at $X = 0$, we have $p_0 = 10^5\ \mathrm{N\,m^{-2}}$, $T_0 = 288\,\mathrm{K}$, $a_0 = 340\,\mathrm{m\,s^{-1}}$, $\gamma = 1.4$, $Pr = 0.72$, $C = 1.47$, $C_T = 1.14$, $\nu_0 = 1.45 \times 10^{-5}\,\mathrm{m^2\,s^{-1}}$, $\nu_{d0} = 3.61 \times 10^{-5}\,\mathrm{m^2\,s^{-1}}$ with $\mu_v/\mu = 0.60$ and $\omega_0/2\pi = 238\,\mathrm{Hz}$. Taking $\varepsilon = \kappa/2 = 0.1$, it follows that $\delta_0 = 0.0180$, $\lambda_0 = 0.00370$, $\delta_{r0} = 0.0532$, $\beta = 1.16 \times 10^{-6}$. For reference, the typical thickness $\sqrt{\nu_0/\omega_0}$ is about 0.1 mm. In the following, we consider the temperature distribution given by

$$H_e = (1 + \tfrac{1}{4}X)^2. \tag{6.11}$$

For $a_0/\kappa\omega_0 l = 1/4$, l corresponds to 4.5 m and the position $x = l$ corresponds to 1.66 for X where the temperature becomes double.

The initial-value problem thus posed is solved numerically. In the case that no temperature gradient is imposed and the term with β is negligible, (5.10) and (5.11) are integrated numerically along the 'characteristics' defined by $\mathrm{d}\theta/\mathrm{d}X = -f$, and if multivaluedness appears in the solution, a discontinuity, i.e. a shock, is fitted into it (Sugimoto 1992). In the present context, however, since we expect no shocks by connecting a suitable array, the usual method of finite difference is employed, which is described briefly. We fix a computation domain in θ and choose grid points separated by $\Delta\theta$ equidistantly with the end points at the lower and upper bounds of the domain.

With f given by $F(\theta)$, (5.11) is first solved for g to yield $G(\theta)$. This is done by solving the integro-differential equation. Once g is available by the method to be described below, we next compute in (5.10) all terms except for $\partial f/\partial X$. The derivatives of integral order are evaluated by central differences. The derivatives of fractional order are evaluated by modifying Simpson's rule. The integral defining the derivative of order α ($\alpha = -1/2$ or $1/2$) is divided into two integrals as follows:

$$\frac{\partial^\alpha f}{\partial \theta^\alpha} = \frac{1}{\sqrt{\pi}} \left(\int_{-\infty}^{\theta-2\Delta\theta} + \int_{\theta-2\Delta\theta}^{\theta} \right) \frac{1}{\sqrt{\theta-\eta}} \frac{\partial^{\alpha+1/2}}{\partial \eta^{\alpha+1/2}} f(\eta) \mathrm{d}\eta, \tag{6.12}$$

the dependence on X being suppressed. The first integral is computed according to Simpson's rule by truncating the lower bound of integration at the lower bound of the computation domain where f and g may be regarded as being essentially zero. When the integral consists of an odd number of intervals of $\Delta\theta$, the trapezoidal rule is applied instead but only to the interval bounded by the lower end. The second integral is calculated analytically by expanding $f(\eta)$ into a quadratic Taylor series around $\eta = \theta$. Then the integral is evaluated by the following formulae for $\alpha = -1/2$ and $\alpha = 1/2$, respectively:

$$\int_{\theta-2\Delta\theta}^{\theta} \frac{f(\eta)}{\sqrt{\theta-\eta}} \mathrm{d}\eta = \left(\frac{8\Delta\theta}{225} \right)^{1/2} [f(\theta-2\Delta\theta) + 8f(\theta-\Delta\theta) + 6f(\theta)] + O(\Delta\theta^{7/2}), \tag{6.13}$$

and

$$\int_{\theta-2\Delta\theta}^{\theta} \frac{1}{\sqrt{\theta-\eta}} \frac{\partial f}{\partial \eta} \mathrm{d}\eta = \left(\frac{2}{9\Delta\theta} \right)^{1/2} [-7f(\theta-\Delta\theta) + 8f(\theta) - f(\theta+\Delta\theta)] + O(\Delta\theta^{5/2}). \tag{6.14}$$

Although the error in (6.14) is worse than in (6.13), it is slightly better than the error involved in the central difference. At the grid point next to the lower end point, the scheme must be modified slightly but the same idea in essence is applied to the interval of width $\Delta\theta$. Thus $\partial f/\partial X$ is now computed and is approximated by the simple forward difference at $X = 0$ and $X = \Delta X$. This yields $f(\theta, \Delta X)$. Updating F by f newly obtained, (5.11) is solved for g at $X = \Delta X$. Repeating the same procedure, the solutions are obtained successively. With f thus available, the integrals I_1 and I_2 are computed according to Simpson's rule by truncating the lower and upper bounds of the integration at the respective bounds of the computation domain.

We now describe the method to solve (5.11). Setting $\partial^2 g/\partial\theta^2 = g''$, the derivative of $3/2$-order of g is rewritten as that of $-1/2$-order of g'', which is solved simultaneously with f and g. Evaluation of (5.11) at a certain grid point, θ say, provides a relation to calculate $g''(\theta)$ in terms of known values at all grid points smaller than θ. The central difference of $g''(\theta)$ thus available gives $g(\theta + \Delta\theta)$ $(= 2g(\theta) - g(\theta - \Delta\theta) + g''(\theta)\Delta\theta^2)$. Advancing in this way, g is solved successively toward the upper bound of the computation domain. In executing this scheme, auxiliary grid points are necessary outside the computation domain to evaluate $\partial f/\partial\theta$, $\partial^2 f/\partial\theta^2$ and $\partial g/\partial\theta$, especially at the upper bound, and the values there are extrapolated by a straight line.

6.1. *An acoustic solitary wave*

We first solve a case where F is prescribed by the solution of the acoustic solitary wave in the lossless case. The solution F is given in the form of the inverse function as

$$-4\tan^{-1}\sqrt{\frac{f_+ - F}{F - f_-}} + \frac{2s}{\sqrt{-f_+ f_-}} \log \left| \frac{[\sqrt{-f_-(f_+ - F)} - \sqrt{f_+(F - f_-)}]^2}{(f_+ - f_-)F} \right| = |\theta|, \tag{6.15}$$

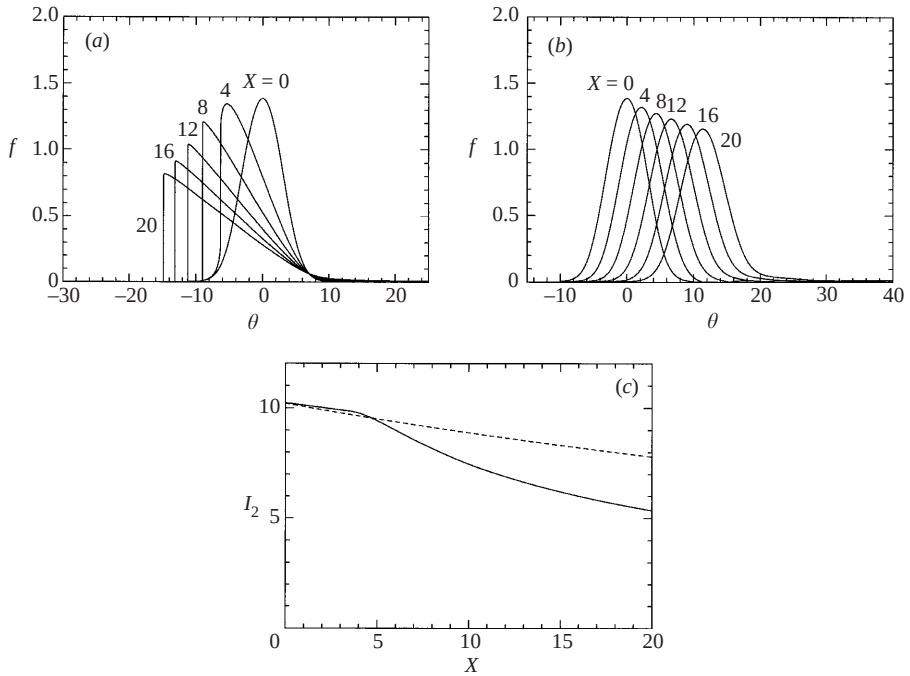

FIGURE 3. Shock and shock-free propagation from the initial profile of the acoustic solitary wave given by (6.15) with $s = 0.5$ in the absence of the temperature gradient where the temporal profiles of f at $X = 0$, 4, 8, 12, 16 and 20 are shown (a) in the tube without the array of Helmholtz resonators and (b) with the array having $\kappa = 0.2$, respectively. (c) The spatial variations of I_2 for cases (a) and (b) shown, respectively, as the solid and broken lines.

with $f_\pm$ defined by

$$f_\pm = -2(s - \tfrac{2}{3}) \pm \sqrt{-\tfrac{4}{3}s + \tfrac{16}{9}}, \tag{6.16}$$

and the signs $\pm$ ordered vertically, where s is a parameter in the range $0 < s < 1$ (Sugimoto 1996). The initial value G is very close to the lossless solution given by $F^2/2 + sF$ because δ_{r0} is small. The initial values of I_1 and I_2 for $f = F$ and $H_e = 1$ at $X = 0$ are given analytically as (Sugimoto 2000)

$$I_1(X = 0) = \int_{-\infty}^{\infty} F \mathrm{d}\theta = 8\sqrt{s(1-s)} + (\tfrac{16}{3} - 4s)\cos^{-1}\frac{(-2+3s)}{\sqrt{4-3s}}, \tag{6.17}$$

and

$$I_2(X = 0) = \int_{-\infty}^{\infty} F^2 \mathrm{d}\theta = 16\sqrt{s(1-s)^3} + \tfrac{8}{3}(1-s)(4-3s)\cos^{-1}\frac{(-2+3s)}{\sqrt{4-3s}}. \tag{6.18}$$

We start by demonstrating the effect of the array of resonators. Without the array being connected, a shock appears and the total energy flux decays significantly by nonlinear damping. In this case, we need only to solve (5.10) with $K = 0$. Figure 3(a) shows the temporal profiles of f evolving from the initial profile given by the solitary wave with $s = 0.5$ in the tube without a temperature gradient $H_e = 1$. The shock emerges at $X \approx 3.5$ and it decays rapidly thereafter. The profiles are computed by the previous method of characteristics with β neglected (Sugimoto 1992). Note in passing that if the temperature distribution (6.11) is given to this tube, the shock formation is delayed.

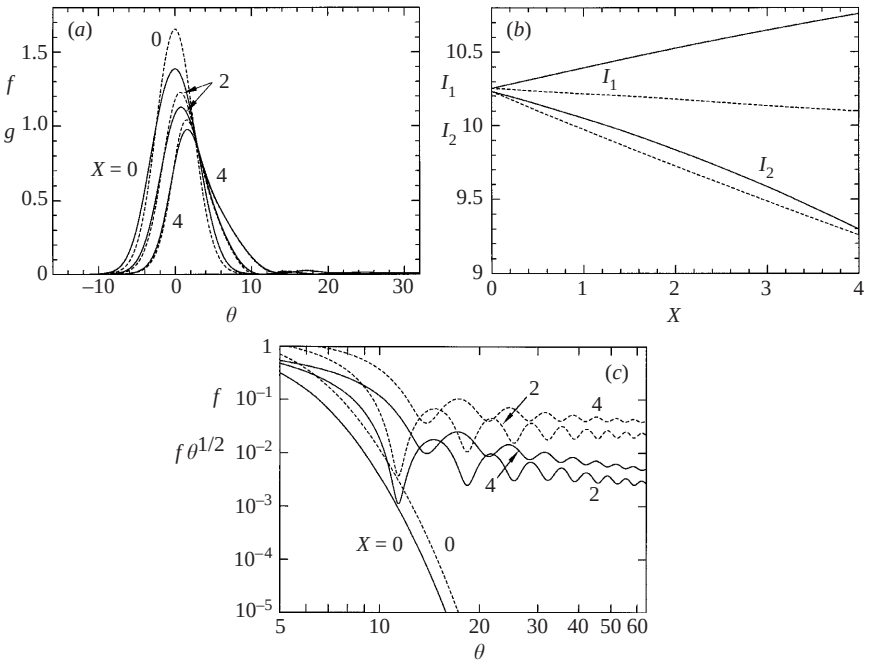

FIGURE 4. Spatial evolution from the initial profile of the acoustic solitary wave given by (6.15) with $s = 0.5$ in the tube with the array of Helmholtz resonators having $\kappa = 0.2$ and in the presence of the temperature distribution $H_e = (1 + X/4)^2$: (*a*) the temporal profiles of f (solid lines) and g (broken lines) at $X = 0, 2$ and 4; (*b*) the spatial variations of I_1 and I_2 as solid lines, with the broken lines representing the absence of the temperature gradient; (*c*) the decay of the tail behind the main pulse plotted logarithmically as f and $f\theta^{1/2}$ versus θ as solid and broken lines, respectively.

The point is estimated from (5.20) to be $X = 4[(1+X_s/8)^2-1]$, X_s being the shock formation point in the case without the temperature gradient. For $X_s \approx 3.5$, it is about 4.3.

When the array of resonators is connected, figure 3(*b*) shows that the profiles remain smooth and therefore the shock is avoided. If all loss effects were ignored, the profile would be translated without any change of form in the positive direction of θ as X increases. In figure 3(*b*), however, the height decreases slowly due to wall friction. Incidentally, it is seen that while the propagation speed of the shock is supersonic, that of the solitary wave is subsonic, because the shock is located in $\theta < 0$ whereas the peak of the solitary wave is located in $\theta > 0$. Figure 3(*c*) shows the spatial variations of I_2. The solid line represents I_2 in the tube without the array and the broken line represents I_2 in the tube with the array. Just after the shock emerges, the solid line drops significantly. This is the onset of nonlinear damping. In the early stage ($X < 4$), however, the decay rate is a little larger for the broken line than for the solid line. This is due to the wall friction at the throat.

Let us now examine the effect of the temperature gradient. Figure 4(*a*) shows the temporal profiles of f and g as the solid and broken lines, respectively, at $X = 0$, 2 and 4 from the initial profile given by the solitary wave with $s = 0.5$ in the presence of the temperature distribution (6.11). It is seen that f decreases, i.e. the pressure p' decreases, almost in accordance with the $-1/4$ power law. In fact, at $X = 4$ where $H_e = 4$ and $H_e^{-1/4} = 1/\sqrt{2} = 0.707$, the peak height is reduced to about 70% of the initial one. As X increases, it is also seen that f and g tend to be equal to each other. This can be understood from (5.11) because H_e (therefore Ω_e in (5.12)) increases as X

increases (Sugimoto & Tsujimoto 2001). Although the pressure decreases, the velocity u increases as $H_e^{1/2}f$ where $H_e^{1/2}$ doubles at $X = 4$. Yet it is not known whether or not the total energy flux increases. Figure 4(b) depicts the spatial variations of I_1 and I_2 as the solid lines where the broken lines represent, for reference, the case without the temperature gradient. With the temperature gradient, the rate of decrease of I_2 becomes slower for $X < 2.3$ than without it, the broken line decaying almost linearly. But no increase can be seen and the total energy flux is not amplified.

The computations are carried out in the domain $-16 \leqslant \theta \leqslant 64$ by taking $\Delta\theta = 0.02$ and $\Delta X = 0.00125$. Because a long tail in θ tends to appear behind the main body of the pulse, the upper bound of the domain is chosen large enough to include as much as possible of the tail. Figure 4(c) plots f and $f\theta^{1/2}$ versus θ on logarithmic scales to show how slowly the tail decays. The solid lines represents f at $X = 0, 2$ and 4. At $X = 0$, since f decrease exponentially, no tail exists. The broken line represents $f\theta^{1/2}$ at the respective values of X. The factor $\theta^{1/2}$ is suggested by the linear theory in Appendix B. Since each broken line appears to approach a constant as θ increases, it is suggested that the decaying behaviour of f is close to $\theta^{-1/2}$ for large values of θ. If this is the case as $\theta \to \infty$, I_1 and I_2 would tend to diverge as the upper bound is taken larger. The values of I_1 and I_2 are compared when taking the upper bound of the domain to be 32, 48 and 64, respectively, with $\Delta\theta$ and ΔX fixed. It is verified that I_1 increases with the upper bound whereas I_2 remains almost unchanged. The latter may be anticipated because the behaviour $\theta^{-1/2}$ for f gives rise to a very weak, logarithmic divergence in I_2. Even if the divergence occurred in a rigorous sense, we are interested in the possibility of amplification of energy flux of the main body of the pulse, and are therefore led to the conclusion that no amplification takes place. In other cases with $s = 0.2$ and 0.8, no amplification is obtained either. Among the three values of s, the rate of decrease in I_2 becomes smaller as s increases.

We checked the accuracy of computations by comparing the values of I_1 and I_2 obtained directly by integrating $H_e^{1/4}f$ and $H_e^{1/2}f^2$ over the entire computation domain of θ, with those obtained by integrating the differential equations (5.24) and (5.25) with respect to X from $X = 0$. When the integrations are limited to a finite range of θ, (5.24) and (5.25) are subjected to modifications due to the contributions from the upper bound in particular. But they are regarded as being comparable with the errors involved. The relative error remains within the order of 10^{-3} at worst. At $X = 0$, the exact values of I_1 and I_2 are $4 + (10/3)\cos^{-1}(-1/\sqrt{10}) \approx 10.30$ whereas the numerical values are 10.23 and 10.25, respectively. Although the accuracy may be improved by taking a finer grid, we are satisfied with this order of error to avoid requiring a large capacity in computation.

We now consider why the energy flux is not amplified. Figure 2 shows the graphs of F for the solitary wave solution with $s = 0.5$ and its fractional derivatives of order $1/2$ and of $-1/2$, drawn as solid, broken and dotted lines, respectively. Using these, figure 5 shows the profile of v_b at $X = 0$, as the solid line, except for the factor outside the parentheses in (5.13), where the first and second terms are drawn as the broken and dotted lines, which correspond to the first and second terms in (5.10), respectively. It is found that v_b is not positive enough to do work on the acoustic main flow. If the temperature gradient is increased, amplification occurs but it soon turns into damping. Further increase in the temperature gradient tends to invalidate the basic assumption that the temperature gradient is gentle. In this connection, we go back to consider physically the situation corresponding to the parameters chosen because the replacement (6.1) might have obscured it. Since ω has been chosen to be ω_0, the meaning of χ has been lost. By the choice (6.11), we have

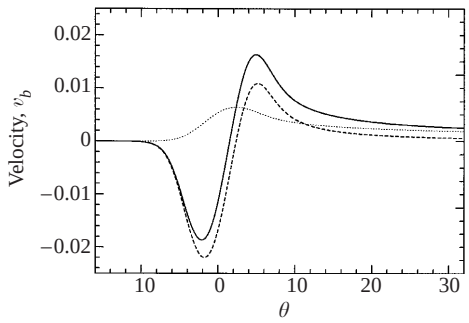

FIGURE 5. Velocity v_b at the edge of the boundary layer at $X = 0$ where the solid line represents the temporal profile of (5.13) except for the factor outside of the parentheses, while the broken and dotted lines represent, respectively, the first and second terms.

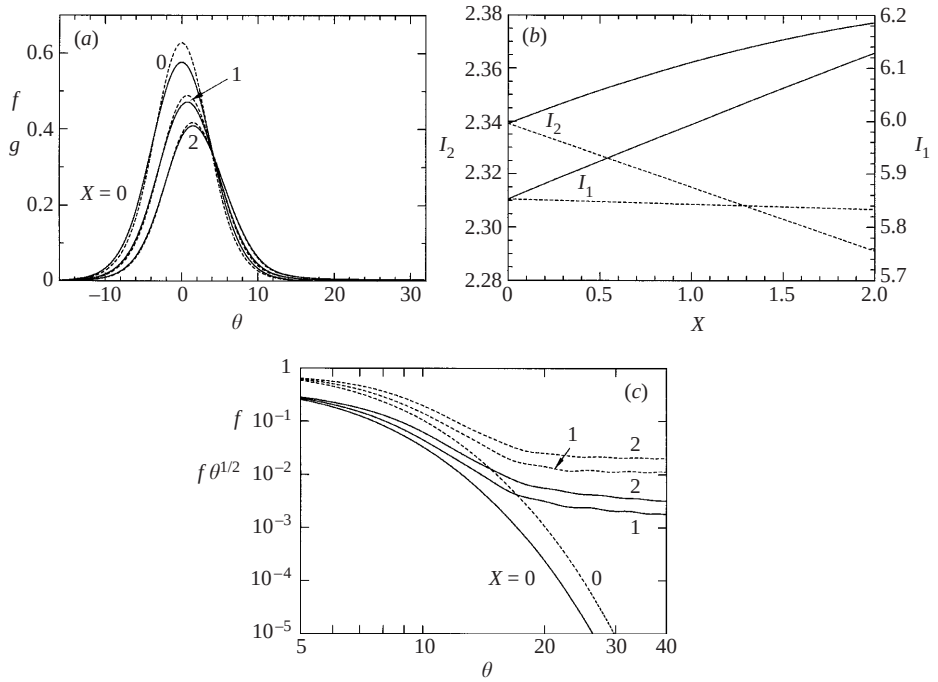

FIGURE 6. Spatial evolution from the initial profile of the acoustic solitary wave given by (6.15) with $s = 0.8$ in the tube with the array of Helmholtz resonators having the larger value of $\kappa = 0.4$ and in the presence of the steeper temperature distribution $H_e = (1 + X/2)^2$: (*a*) the temporal profiles of f (solid lines) and g (broken lines) at $X = 0, 1$ and 2; (*b*) the spatial variations of I_1 and I_2 as the solid lines, with the broken lines representing the absence of the temperature gradient; (*c*) the decay of the tail behind the main pulse plotted logarithmically as f and $f\theta^{1/2}$ versus θ as solid and broken lines, respectively.

$a_0/\omega_0 l = (a_0/\omega l)\omega/\omega_0 = \kappa/4$. If a typical angular frequency ω for the solitary wave is defined as an inverse of a half-width, ω_0/ω becomes about 8 for $s = 0.5$ (Sugimoto 1996). Thus it is found that $\chi(= a_0/\omega l)$ takes the value 0.4 so that the ratio $\chi/\varepsilon = 4$.

As the results so far obtained are contrary to our expectation, we now look for the possibility of amplification by changing conditions of the tube. For amplification, a consideration based on (5.26) and (5.27) suggests that while χ should be taken larger,

of course, $\partial f/\partial\theta$ should be made small. In this respect, the choice of a large values of s is preferable because the height of the solitary wave (f_+ in (6.16)) becomes lower as s increases so that the magnitude of $\partial f/\partial\theta$ becomes smaller. Also, the choice of a large value of ε, i.e. κ, is preferable to reduce δ_e for the friction loss. So we consider a case where s is chosen to be 0.8, while κ is increased to 0.4 so that $\varepsilon = 0.2$. Furthermore we impose the steeper temperature gradient given by $H_e = (1 + X/2)^2$. Figure 6 shows the results corresponding to figure 4. The computations are carried out in the domain $-20 \leqslant \theta \leqslant 40$ with $\Delta\theta = 0.01$ and $\Delta X = 0.00125$. The quantitative behaviour in figures 6(a) and 6(c) is similar to figures 4(a) and 4(c), respectively. But figure 6(b) indicates that I_2 at $X = 2$ (the solid line) increases by about 1.5% of the initial value, whereas I_2 decreases by about 2% when no temperature gradient is imposed (the broken line). This demonstrates that the energy of the acoustic solitary wave can be amplified by choosing suitable conditions. It is revealed, however, that because the solitary wave has a fixed profile for a given value of s, it is a delicate matter to fulfil the conditions for amplification. For this, initial profiles should have some degrees of freedom. In passing, we note the error involved in the computations. At $X = 0$, the exact values of I_1 and I_2 are $3.2 + (6.4/3)\cos^{-1}(1/\sqrt{10}) \approx 5.865$ and $1.28 + (2.56/3)\cos^{-1}(1/\sqrt{10}) \approx 2.346$, respectively, whereas the numerical values are 5.853 and 2.339, respectively. There is accompanied by the relative error of order of 10^{-3}. In view of this, the amplification is meaningful.

6.2. *A square pulse*

Next we solve the evolution from a smoothed square pulse given by

$$F(\theta) = \frac{1}{2}\left[\tanh\left(\frac{\theta}{b} + \frac{\tau}{2}\right) - \tanh\left(\frac{\theta}{b} - \frac{\tau}{2}\right)\right], \tag{6.19}$$

where b (> 0) corresponds to $\sqrt{\Omega_0}$ and the duration $b\tau$ (> 0) is left as an adjustable parameter. For $b \gg 1$, the profile of G is almost identical to that of F. The integrals I_1 and I_2 at $X = 0$ are calculated, respectively, to be

$$I_1(X=0) = \int_{-\infty}^{\infty} F\mathrm{d}\theta = b\log\left[\frac{1+\tanh(\frac{1}{2}\tau)}{1-\tanh(\frac{1}{2}\tau)}\right] \approx b\tau \quad \text{for } \tau \gg 1, \tag{6.20}$$

and

$$I_2(X=0) = \int_{-\infty}^{\infty} F^2\mathrm{d}\theta = \tfrac{1}{2}b\tau[\tanh(\tfrac{1}{2}\tau) + \coth(\tfrac{1}{2}\tau)] - b \approx b(\tau - 1) \quad \text{for } \tau \gg 1. \tag{6.21}$$

First we show the evolution from the pulse with $b = 8$ and $\tau = 10$ in the tube without the temperature gradient. The choice of the large value of b is suggested by the previous finding that no shock emerges if $\Omega_0 \gg 1$ (Sugimoto 1992). Of course without the array connected, the shock is formed at $X \approx 2b = 16$. As b becomes smaller, it occurs at a position closer to $X = 0$. The total energy flux of the square pulse chosen is about seven times larger than that of the acoustic solitary wave shown in figure 4. Because the evolution from this pulse is qualitatively the same as that shown in figure 3, we proceed to consider the case with the array of resonators having $\kappa = 0.2$. Figure 7(a) depicts the temporal profiles of f at $X = 0, 16$ and 32 in the absence of the temperature gradient. No profiles of g are drawn because $f \approx g$. No shock is seen to emerge, and instead the pulse tends to oscillate as X increases. It is suspected that the oscillations will eventually split into a sequence of solitary waves.

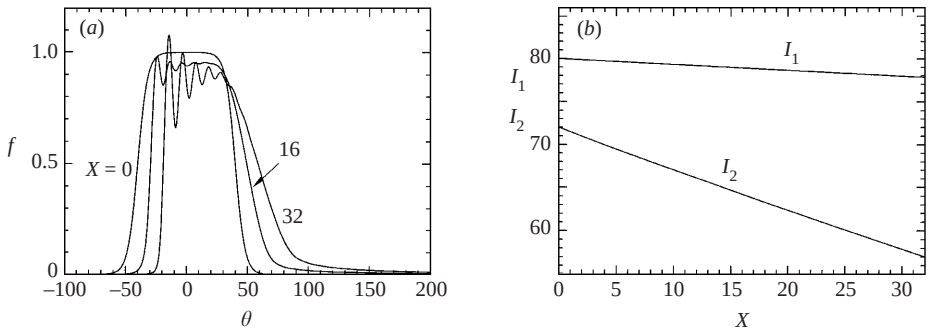

FIGURE 7. Spatial evolution from the initial profile given by the square pulse (6.19) with $b = 8$ and $\tau = 10$ in the tube with the array of Hemholtz resonators having $\kappa = 0.2$ and in the absence of the temperature gradient: (a) the temporal profiles of f at $X = 0$, 16 and 32; and (b) the spatial variations of I_1 and I_2.

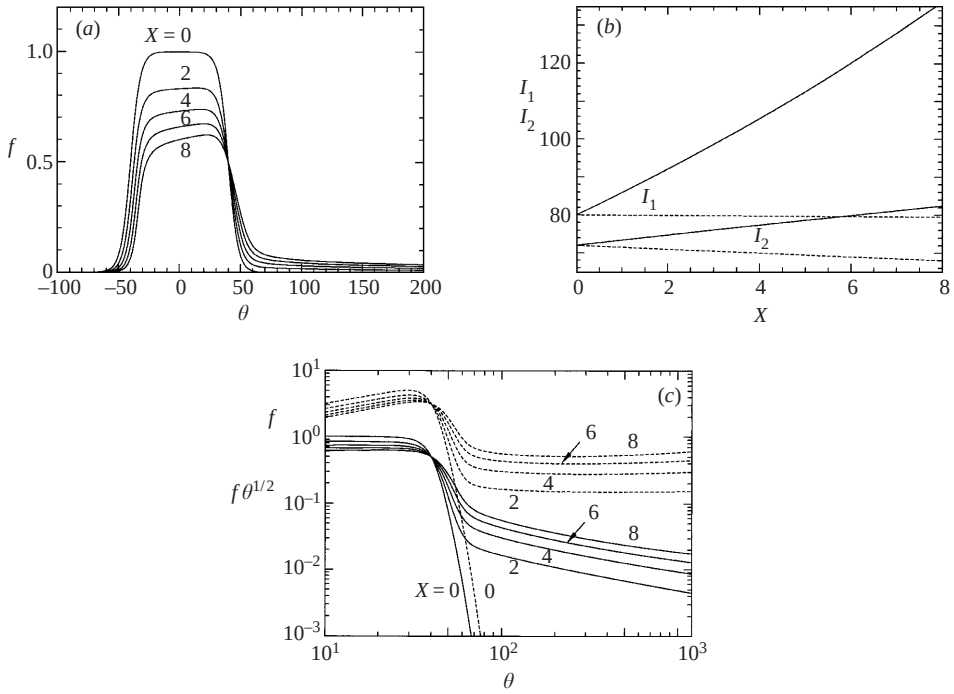

FIGURE 8. Spatial evolution from the initial profile given by the square pulse (6.19) with $b = 8$ and $\tau = 10$ in the tube with the array of resonators having $\kappa = 0.2$ and in the presence of the temperature distribution $H_e = (1 + X/4)^2$: (a) the temporal profiles of f at $X = 0, 2, 4, 6$ and 8; (b) the spatial variations of I_1 and I_2 as solid lines, with the broken lines representing the absence of the temperature gradient; (c) the decay of the tail behind the main pulse plotted logarithmically as f and $f\theta^{1/2}$ versus θ as solid and broken lines, respectively.

Figure 7(b) shows the spatial variations of I_1 and I_2. The decay of I_2 is seen to be gentle and almost linear.

When the temperature distribution (6.11) is imposed in the tube with $\kappa = 0.2$, the profiles change more rapidly in the early stage of evolution. Figure 8(a) shows the temporal profiles of f at $X = 0$, 2, 4, 6 and 8 for $b = 8$ and $\tau = 10$. The height of the square pulse decrease as X increases. In this case as well it is found that the height

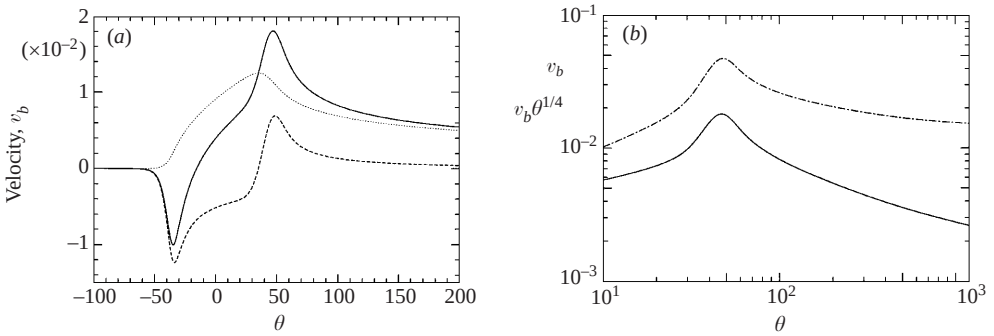

FIGURE 9. Velocity v_b at the edge of the boundary layer at $X = 4$: (a) the temporal profile of (5.13) (solid line) except for the factor outside the parentheses taking the value $0.50\,\mathrm{m\,s^{-1}}$, while the broken and dotted lines represent, respectively, the first and second terms; (b) logarithmic-scale plots of v_b and $v_b\theta^{1/4}$, v_b without the factor, versus θ as solid and chain lines, respectively.

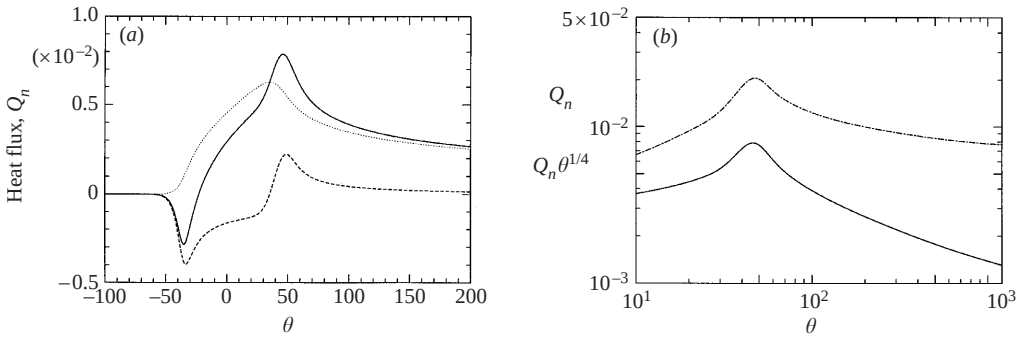

FIGURE 10. Heat flux Q_n into the boundary layer from the wall at $X = 4$ where (a) shows, in the solid line, the temporal profile of (5.14) except for the factor outside of the square brackets taking the value $1.7 \times 10^2\,\mathrm{kW\,m^{-2}}$, while the broken and dotted lines represent, respectively, the first and second terms, and (b) logarithmic-scale plots of Q_n and $Q_n\theta^{1/4}$, Q_n without the factor, versus θ as solid and chain lines, respectively.

of the pulse at $\theta = 0$ obeys the $-1/4$ power law of H_e roughly. Figure 8(b) shows the spatial variations of I_1 and I_2 up to $X = 8$ where the broken lines represent, for reference, those in the absence of the temperature gradient, $H_e = 1$. It is found that I_2 increases from 72 to about 77 at $X = 4$, i.e. about 7%, whereas I_1 increases considerably. The smaller increase in I_2 is brought about by the wall friction on the throat wall, i.e. due to the term associated with g in (5.25). The computations are carried out in the domain $-100 \leqslant \theta \leqslant 1200$ with $\Delta\theta = 0.4$ and $\Delta X = 0.01$. Computing in a smaller domain $-100 \leqslant \theta \leqslant 600$, shows that I_1 changes with the upper bound whereas I_2 remains almost unchanged. Figure 8(c) shows the decay of the tail by plotting f and $f\theta^{1/2}$ versus θ, in logarithmic scales, as the solid and broken lines, respectively. In this case as well, since f seems to decay as $\theta^{-1/2}$, I_2 may tend to diverge in the rigorous sense as the upper bound is taken larger. But because I_2 increases without taking any account of the tail outside the domain, we may conclude that the energy flux of the main body of the pulse is amplified by the temperature gradient.

Here we check the variations of v_b graphically. Figure 9(a) displays the temporal profile of v_b at $X = 4$ as the solid line, except for the factor outside the parentheses of

(5.13), where the broken and dotted lines represent, respectively, the first and second terms. The factor outside the parentheses takes the value $0.50\,\mathrm{m\,s^{-1}}$ for $\varepsilon = \kappa/2 = 0.1$ and $\omega/2\pi = \omega_0/2\pi = 238\,\mathrm{Hz}$. Because the pulse width is much larger than that of the solitary wave and $\partial f/\partial\theta$ almost vanishes in the plateau region of f, it is evident that the condition for amplification is easily met. Figure 9(b) shows the decaying behaviour of v_b at $X = 4$ for a large value of θ by logarithmic plots of v_b and $v_b\theta^{1/4}$ versus θ, as the solid and chain lines, respectively, v_b without the factor. It appears that v_b decays very slowly and close to $\theta^{-1/4}$ for large values of θ. This behaviour is mainly contributed from the second term in (5.13) because the first term appears to decay close to $\theta^{-3/2}$.

We also show in figure 10(a) the heat flux at $X = 4$ where the solid line represents the profile of (5.14) except for the factor outside of the square brackets, while the broken and dotted lines represent, respectively, the first and second terms. The factor takes the value $1.7\times10^2\,\mathrm{kW\,m^{-2}}$.The coefficients $(C-1)/C$ and $(C+4C_T-3)/(C+4C_T)$ take the values 0.32 and 0.50, respectively, and the ratio is about 1 to 1.6. Comparing this with (5.13), it is found that the effect of the temperature gradient (second term) appears stronger for Q_n than for v_b. In consequence, the maximum in Q_n appears greater than that in v_b in relation to the respective minimum while Q_n switches to be positive earlier than v_b. But it may be said that Q_n is almost in phase with v_b. Finally we note the decaying behaviour of Q_n at $X = 4$ for a large value of θ. Figure 10(b) shows logarithmic plots of Q_n and $Q_n\theta^{1/4}$ versus θ, as the solid and chain lines, respectively, Q_n without the factor. This behaviour is quantitatively the same, of course, as that of v_b. If the asymptotic behaviour as $\theta \to \infty$ is close to $\theta^{-1/4}$, it results that an infinite amount of heat flows into the boundary layer in total.

7. Conclusion

The propagation of nonlinear acoustic waves in a gas-filled tube under a temperature gradient has been formulated by taking account of the boundary layer and of an array of Helmholtz resonators. The mechanism of amplification of the energy flux is elucidated from the standpoint of the action of the boundary layer. Also demonstrated is the merit of the use of array of resonators to avoid the undesirable loss of an energy flux associated with the emergence of a shock. When the temperature gradient is positive and appropriate, the boundary layer can 'pinch' the acoustic main flow, to pump energy into the waves. By deriving the nonlinear wave equations for unidirectional propagation, the evolution of the acoustic solitary wave and of the square pulse has been examined and the spatial variations of the total energy flux have been obtained. It is revealed that the total energy flux can indeed be amplified against the intrinsic loss.

In the case of an acoustic solitary wave, however, the result is negative in the tube with the array having $\kappa = 0.2$ chosen as a first attempt. Comparing with the case of the square pulse, one reason is that once the tube is chosen, i.e. κ is fixed, the form of the solitary wave is uniquely determined by the value of s and no other free parameters are involved. For a given temperature gradient, therefore, it can occur that the condition of amplification is not met for any value of s. Then the geometry of the tube must be modified. In fact, when κ is increased to 0.4 and a steeper temperature gradient is imposed, it is found that amplification of the energy flux takes place. Note in passing that there are combinations of κ and a temperature distribution such that the total energy flux is almost maintained at the initial value over a large value of X. For example, this is the case of the solitary wave with $s = 0.8$ in the tube with the

array having $\kappa = 0.2$ and the temperature gradient $H_e = (1 + X/2)^2$. In view of these results, the choice of the geometry of the tube for a given temperature gradient is found to be crucial to the amplification of energy flux of the acoustic solitary wave.

For simplicity in elucidation of the mechanism of amplification, we have assumed that there are none of the stacks usually employed in thermoacoustic heat engines. Even without use of the stacks, it is shown that the thermoacoustic effects can amplify the energy flux. Their use will enhance the amplification substantially by increasing δ_e and λ_e as though the tube diameter were smaller. To achieve further amplification, C_T should be taken larger and C smaller by selecting a gas having γ close to unity and a smaller value of Pr.

Imagine that a temperature gradient, positive and negative, is imposed along a looped tube and that a compression pulse is propagated around the tube unidirectionally. If the pulse could gain energy after one turn, it follows that the pulse has received heat to transform it into kinetic and potential energy. Furthermore if this process could be repeated cyclically by extracting the energy gained and reshaping the pulse, this is a thermoacoustic prime mover utilizing the pulse. Of course, instead of the pulse, we may exploit a continuous wavetrain propagating unidirectionally. In reality, the pulse will be used in an initial 'ignition' process and it will eventually transform into the wavetrain. In any event, to gain more output, the pressure level is required to be set higher. Then emergence of a shock will be inevitable, especially where the gradient is negative. The combined use with an array of Helmholtz resonators is expected to resolve the problem.

The authors would like to thank the referees for their valuable comments. This work has been supported by the Grants-in-Aid from the Japan Society for the Promotion of Science and also from The Mitsubishi Foundations, Tokyo, Japan.

Appendix A. Explicit form of the boundary-layer solutions

Here, we describe briefly the method to solve (4.17) and (4.18) under the boundary conditions (4.19) and the matching conditions (4.20). Defining the transform by a caret, for example,

$$\mathscr{F}\{u\} \equiv \frac{1}{\sqrt{2\pi}} \int_{-\infty}^{\infty} u(x,t) \exp(\mathrm{i}\omega t)\mathrm{d}t \equiv \hat{u}(x,\omega), \tag{A 1}$$

(4.17) is solved to yield

$$\hat{\tilde{u}} = -\hat{u}E_1, \tag{A 2}$$

where E_1, and E_2 below, are defined, respectively, by

$$E_1 = \exp[-(\sigma/v_e)^{1/2}n], \quad E_2 = \exp[-(Pr\sigma/v_e)^{1/2}n], \tag{A 3}$$

with $\sigma = -\mathrm{i}\omega$ and the real part of $\sigma^{1/2}$ is taken positive. Similarly, (4.18) is solved as

$$\hat{\tilde{T}} = -(\hat{T} - \hat{T}_e)E_2 + \frac{Pr}{(1-Pr)} \frac{\mathrm{d}T_e}{\mathrm{d}x} \frac{\hat{u}}{\sigma}(E_2 - E_1). \tag{A 4}$$

The Fourier transform of v_b is calculated by

$$\hat{v_b} = \int_0^{\infty} \left[\sigma \left(\frac{\hat{\tilde{T}}}{T_e} \right) - \frac{\partial \hat{\tilde{u}}}{\partial x} + \frac{1}{T_e} \frac{\mathrm{d}T_e}{\mathrm{d}x} \hat{\tilde{u}} \right] \mathrm{d}n. \tag{A 5}$$

Substituting (A 2) and (A 4) into (A 5), and integrating with respect to n, $\hat{v_b}$ is obtained as

$$\hat{v_b} = -\frac{\sqrt{v_e}}{\sqrt{Pr}}\sigma^{1/2}\left(\frac{\hat{T}-\hat{T}_e}{T_e}\right) + \sqrt{v_e}\sigma^{-1/2}\frac{\partial \hat{u}}{\partial x} + \left(\frac{1}{2} - \frac{1}{1+\sqrt{Pr}}\right)\frac{\sqrt{v_e}}{T_e}\frac{\mathrm{d}T_e}{\mathrm{d}x}\sigma^{-1/2}\hat{u}, \quad \text{(A 6)}$$

where use has been made of the relations $v_e^{-1}\mathrm{d}v_e/\mathrm{d}x = T_e^{-1}\mathrm{d}T_e/\mathrm{d}x$,

$$\frac{\partial E_1}{\partial x} = \frac{1}{2T_e}\frac{\mathrm{d}T_e}{\mathrm{d}x}\left(\frac{\sigma}{v_e}\right)^{1/2} nE_1, \quad \int_0^\infty \frac{\partial E_1}{\partial x}\mathrm{d}n = \frac{1}{2T_e}\frac{\mathrm{d}T_e}{\mathrm{d}x}\left(\frac{\sigma}{v_e}\right)^{-1/2}. \quad \text{(A 7)}$$

Using (4.9) to replace the temperature, we have

$$\hat{v_b} = \left(1 + \frac{\gamma-1}{\sqrt{Pr}}\right)\sqrt{v_e}\sigma^{-1/2}\frac{\partial \hat{u}}{\partial x} + \left(\frac{1}{2} + \frac{1}{\sqrt{Pr}+Pr}\right)\frac{\sqrt{v_e}}{T_e}\frac{\mathrm{d}T_e}{\mathrm{d}x}\sigma^{-1/2}\hat{u}. \quad \text{(A 8)}$$

To make an inverse transform, we note the following formula:

$$\mathscr{F}\left\{\frac{\partial^\alpha u}{\partial t^\alpha}\right\} = \sigma^\alpha \hat{u}, \quad \text{(A 9)}$$

where $\alpha = -1/2$ or $1/2$. Using this formula, we obtain immediately v_b in the form of (4.22). The temperature gradient at $n = 0$ is also obtainable as

$$\left.\frac{\partial \hat{\hat{T}}}{\partial n}\right|_{n=0} = \frac{\sqrt{Pr}}{\sqrt{v_e}}\left[\sigma^{1/2}(\hat{T}-\hat{T}_e) + \frac{\sqrt{Pr}}{1+\sqrt{Pr}}\frac{\mathrm{d}T_e}{\mathrm{d}x}\sigma^{-1/2}\hat{u}\right]. \quad \text{(A 10)}$$

Using (4.9), (A 10) is alternatively written in terms of $\hat{u}$ alone as

$$\left.\frac{\partial \hat{\hat{T}}}{\partial n}\right|_{n=0} = -\frac{\sqrt{Pr}}{\sqrt{v_e}}\left[(\gamma-1)T_e\sigma^{-1/2}\frac{\partial \hat{u}}{\partial x} + \frac{1}{1+\sqrt{Pr}}\frac{\mathrm{d}T_e}{\mathrm{d}x}\sigma^{-1/2}\hat{u}\right]. \quad \text{(A 11)}$$

Appendix B. Linear initial-value problem

In order to examine the asymptotic behaviour of the tail, it is instructive to consider solutions to the linearized equations of (5.10) and (5.11) under the initial conditon given by $f(\theta, X=0) = \delta(\theta)$, $\delta(\theta)$ being the delta function. The temperature distribution is assumed to be given by

$$H_e = \left(1 + \frac{X}{m}\right)^2, \quad \text{(B 1)}$$

where m ($\neq 0$) is an arbitrary constant. We set f and g to be $H_e^{-1/4}\varphi(\theta, X)$ and $H_e^{-1/4}\psi(\theta, X)$, respectively, to remove the lossless effect of the temperature gradient. Rewriting (5.10) linearized, and (5.11) in terms of φ and ψ, and using (6.5) and $\Omega_e/\Omega_0 = H_e$, it follows that

$$\frac{\partial \varphi}{\partial X} = -\delta_0\left(1 + \frac{X}{m}\right)\frac{\partial^{1/2}\varphi}{\partial \theta^{1/2}} + \frac{2\lambda_0}{m}\frac{\partial^{-1/2}\varphi}{\partial \theta^{-1/2}} - K\frac{\partial \psi}{\partial \theta}, \quad \text{(B 2)}$$

and

$$\frac{\partial^2 \psi}{\partial \theta^2} + \delta_{r0}\left(1 + \frac{X}{m}\right)\frac{\partial^{3/2}\psi}{\partial \theta^{3/2}} + \Omega_0\left(1 + \frac{X}{m}\right)^2\psi = \Omega_0\left(1 + \frac{X}{m}\right)^2\varphi. \quad \text{(B 3)}$$

Applying to (B 3) the Fourier transform with respect to θ (whose definition is given by (A 1) with t replaced by θ), $\hat{\psi}(\omega, X)$ is expressed in terms of $\hat{\varphi}(\omega, X)$ as $\Omega_0(1+X/m)^2\hat{\varphi}/D(\omega, X)$, where D is defined as

$$D(\omega, X) = \Omega_0\left(1+\frac{X}{m}\right)^2 + \delta_{r0}(-\mathrm{i}\omega)^{3/2}\left(1+\frac{X}{m}\right) - \omega^2. \tag{B 4}$$

With $\hat{\psi}$ substituted into (B 2) as transformed, and $\hat{\varphi}(\omega, 0) = 1/\sqrt{2\pi}$, $\hat{\varphi}$ is solved as

$$\hat{\varphi} = \frac{1}{\sqrt{2\pi}}\left[\frac{D(\omega,0)}{D(\omega,X)}\right]^{\alpha_1}\left[\frac{W(\omega,0)}{W(\omega,X)}\right]^{\alpha_2} \times \exp\left[-\delta_0(-\mathrm{i}\omega)^{1/2}\left(X+\frac{X^2}{2m}\right) + \frac{2\lambda_0}{m}(-\mathrm{i}\omega)^{-1/2}X + \mathrm{i}K\omega X\right], \tag{B 5}$$

where $W(\omega, X)$ is defined as

$$W(\omega, X) = \frac{D^+(\omega, X)}{D^-(\omega, X)} = \frac{2\Omega_0(1+X/m) + \delta_{r0}(-\mathrm{i}\omega)^{3/2} + (4\Omega_0\omega^2 + \mathrm{i}\delta_{r0}^2\omega^3)^{1/2}}{2\Omega_0(1+X/m) + \delta_{r0}(-\mathrm{i}\omega)^{3/2} - (4\Omega_0\omega^2 + \mathrm{i}\delta_{r0}^2\omega^3)^{1/2}}, \tag{B 6}$$

with $D^+D^- = 4\Omega_0 D$, and α_1 and α_2 given by

$$\alpha_1 = \frac{mK\delta_{r0}}{2\sqrt{2}\Omega_0}|\omega|^{5/2}(1-\mathrm{isgn}\omega) \quad \text{and} \quad \alpha_2 = \frac{\mathrm{i}mK\omega^3(2\Omega_0 + \mathrm{i}\delta_{r0}^2\omega)}{2\Omega_0(4\Omega_0\omega^2 + \mathrm{i}\delta_{r0}^2\omega^3)^{1/2}}, \tag{B 7}$$

with $(-\mathrm{i}\omega)^{\pm 1/2} = (1 \mp \mathrm{isgn}\omega)|\omega|^{\pm 1/2}/\sqrt{2}$, the signs ordered vertically, and $(-\mathrm{i}\omega)^{3/2} = -(1+\mathrm{isgn}\omega)|\omega|^{3/2}/\sqrt{2}$.

With $\hat{\varphi}$ available, the integrals of φ $(= H_e^{1/4}f)$ and φ^2 $(= H_e^{1/2}f^2)$ over the whole range of θ are obtained, respectively, by

$$\int_{-\infty}^{\infty}\varphi\ \mathrm{d}\theta = \lim_{\omega\to 0}\sqrt{2\pi}\hat{\varphi}(\omega, X), \tag{B 8}$$

and by Parseval formula

$$\int_{-\infty}^{\infty}\varphi^2\mathrm{d}\theta = \int_{-\infty}^{\infty}|\ \hat{\varphi}\ |^2\mathrm{d}\omega. \tag{B 9}$$

Examining the asymptotic behaviours of $\hat{\varphi}$ as $\omega \to 0$ and $|\omega| \to \infty$, it is found that when m is positive, both integrals on the right-hand sides diverge due to the contribution of $\exp[2\lambda_0(-\mathrm{i}\omega)^{-1/2}X/m]$ from the vicinity of $\omega = 0$ for $X > 0$. Hence I_1 and I_2 become infinite in the case of the positive temperature gradient.

Although the full inversion of $\hat{\varphi}$ is difficult to execute, we look at how the integrals diverge. Because the divergence is due to the second term on the right-hand side of (B 2), we consider, for simplicity, the case without the array, i.e. $K = \alpha_1 = \alpha_2 = 0$. Assuming that $\lambda_0 \ll \delta_0$, (B 2) is solved in terms of the asymptotic expansion of λ_0 by setting $\varphi = \varphi_0 + \lambda_0\varphi_1 + \ldots$. Then $\hat{\varphi}_0$ is given by $(1/\sqrt{2\pi})\exp[-\delta_0(X+X^2/2m)(-\mathrm{i}\omega)^{1/2}]$. Using the formulae (see Oberhettinger 1957, pp. 27 and 138), this is inverted to yield

$$\varphi_0 = \frac{\delta_0(X+X^2/2m)}{2\sqrt{\pi}|\theta|^{3/2}}\exp\left[-\frac{\delta_0^2(X+X^2/2m)^2}{4|\theta|}\right]h(\theta), \tag{B 10}$$

where $h(\theta)$ is a unit step function. It is found that through wall friction, the initial delta function spreads backward ($\theta > 0$) to form a tail decreasing monotonically as $\theta^{-3/2}$. Yet the integral of φ_0 is preserved at the initial value of unity whereas that of φ_0^2 remains finite for $X > 0$ but decays as X increases, although the integral of φ^2

cannot be defined at $X = 0$ or may be interpreted to be infinite. Proceeding to the first-order problem, $\hat{\varphi}_1$ is given by $(2X/m)(-\mathrm{i}\omega)^{-1/2}\hat{\varphi}_0$, which may also be obtainable from the formal expansion of the second factor in the exponential of (B 5). This can be transformed inversely by using the formulae (Oberhettinger 1957, pp. 27 and 139) to

$$\varphi_1 = \frac{2X}{m}\frac{\partial^{-1/2}\varphi_0}{\partial\theta^{-1/2}} = \frac{2X}{\sqrt{\pi}m|\theta|^{1/2}}\exp\left[-\frac{\delta_0^2(X + X^2/2m)^2}{4|\theta|}\right]h(\theta). \tag{B 11}$$

This shows that the temperature gradient yields a tail which decreases as $\theta^{-1/2}$ more slowly than that due to the wall friction. The tail of $\theta^{-1/2}$ will make I_1 and I_2 diverge. But note that the asymptotic solution thus obtained is not uniformly valid as $\theta \to \infty$ because $\lambda\varphi_1$ becomes comparable with φ_0 or larger than it. On the other hand, when m is negative, (B 8) and (B 9) indicate that the integrals of the full solution converge. In this case, some cancellations occur to yield finite values of the integrals.

REFERENCES

Abramowitz, M. & Stegun, I. A. 1972 *Handbook of Mathematical Functions*. Dover.

Backhaus, S. & Swift, G. W. 1999 A thermoacoustic Stirling heat engine. *Nature*. **399**, 335–338.

Chester, W. 1964 Resonant oscillations in closed tubes. *J. Fluid Mech.* **18**, 44–64.

Howe, M. S. 1998 *Acoustics of Fluid-Structure Interactions*. Cambridge University Press.

Kirchhoff, G. 1868 Über den Einfluss der Wärmeleitung in einem Gase auf die Schallbewegung. *Ann. Phys. Chem.* **134**, 177–193.

Oberhettinger, F. 1957 *Tabellen zur Fourier Transformation*. Springer.

Pierce, A. D. 1991 *Acoustics. An Introduction to Its Physical Principles and Applications*. Acoustical Society of America.

Rayleigh, Lord 1945 *The Theory of Sound*. Vol. II. pp. 230–234. Dover

Rott, N. 1969 Damped and thermally driven acoustic oscillations in wide and narrow tubes. *Z. Angew. Math. Phys.* **20**, 230–243.

Rott, N. 1973 Thermally driven acoustic oscillations. Part II: stability limit for helium. *Z. Angew. Math. Phys.* **24**, 54–72.

Rott, N. 1980 Thermoacoustics. *Adv. Appl. Mech.* **20**, 135–175.

Sugimoto, N. 1989 'Generalized' Burgers equations and fractional calculus. In *Nonlinear Wave Motion* (ed. A. Jeffrey), pp. 162–179. Longman.

Sugimoto, N. 1992 Propagation of nonlinear acoustic waves in a tunnel with an array of Helmholtz resonators. *J. Fluid Mech.* **244**, 55–78.

Sugimoto, N. 1996 Acoustic solitary waves in a tunnel with an array of Helmholtz resonators. *J. Acoust. Soc. Am.* **99**, 1971–1976.

Sugimoto, N. 2000 Mass, momentum, and energy transfer by the propagation of acoustic solitary waves. *J. Acoust. Soc. Am.* **107**, 2398–2405.

Sugimoto, N., Masuda, M., Ohno, J. & Motoi, D. 1999 Experimental demonstration of generation and propagation of acoustic solitary waves in an air-filled tube. *Phys. Rev. Lett.* **83**, 4053–4056.

Sugimoto, N. & Tsujimoto, K. 2001 Effects of temperature gradient on the propagation of an acoustic solitary wave in an air-filled tube. In *IUTAM Symp. on Diffraction and Scattering in Elasticity and Fluid Mechanics* (ed. I. D. Abrahams). Kluwer, in press.

Swift, G. W. 1988 Thermoacoustic engines. *J. Acoust. Soc. Am.* **84**, 1145–1180.

Swift, G. W. 1995 Thermoacoustic engines and refrigerators. *Phys. Today*, **48**, 22–28.

Wheatley, J. C. 1986 Intrinsically irreversible or natural engines. In *Proc. Intl School of Phys. Enrico Fermi: Frontiers in Physical Acoustics* (ed. D. Sette), pp. 395–475. North-Holland.

Yazaki, T., Iwata, A., Maekawa, T. & Tominaga, A. 1998 Traveling wave thermoacoustic engine in a looped tube. *Phys. Rev. Lett.* **81**, 3128–3131.